Simulation of glacierized headwater catchments in the Swiss Alps with climate model data

Judith Meyer

Master thesis at the
Chair of Environmental Hydrological Systems,
Albert-Ludwigs-University, Freiburg
supervised by Prof. Dr. Kerstin Stahl and Prof. Dr. Jan Seibert.

Freiburg i. Br., September 2017

Master thesis

01. April 2017 - 30. September 2017

Simulation of glacierized headwater catchments in the Swiss Alps with climate model data

At the
Chair of Environmental Hydrological Systems,
Faculty of Environment and Natural Resources,

Albert-Ludwigs-University
Friedrichstraße 39, 79098 Freiburg im Breisgau

Judith Meyer
Candidate M.Sc. Hydrology
Matriculation Number: 4106369
4. Semester
SS 2017
E-Mail: judith.meyer@jupiter.uni-freiburg.de

First supervisor:	Prof. Dr. Kerstin Stahl
Second supervisor:	Prof. Dr. Jan Seibert
Research supervisor:	Irene Kohn

Freiburg i. Br., 29. September 2017

Acknowledgements

I would like to thank:

- Prof. Dr. Kerstin Stahl, University of Freiburg, and Prof. Dr. Jan Seibert, University of Zürich, for constructively supervising my thesis, giving valuable comments and research directions.

- Irene Kohn, University of Freiburg, for the HBV set-up and calibration as well as patiently explaining the HBV-light model.

- Dr. Alex J. Cannon, research scientist at the Government of Canada, for kindly helping me with the set-up of the bias correction and providing his R-package MBC (version 0.10-1, Cannon (2016*a*)).

- Kirsti Hakala, PhD student at the University of Zürich, for generously providing me the prepared RCM output for this study's catchments.

Contents

List of Figures

List of Tables

List of Abbreviations

Abbreviation	Unit	Name
ASG Rhine		Project studying the streamflow components of snow and glacier melt of the River Rhine (German: Abflussanteile aus Schnee- und Gletscherschmelze im Rhein) (Stahl et al. 2016)
BC		Bias correction
BfG		German Federal Institute of Hydrology (German: Bundesanstalt für Gewässerkunde)
DWD		Germany's National Meteorological Service (German: Deutscher Wetterdienst)
FOEN		Swiss Federal Office for the Environment
HBV		Conceptual, semi-distributed hydrological model (Swedish: Hydrologiska Byråns Vattenbalansavdelning)
HBV-light		HBV model version currently developed at the University of Zurich
HYRAS		Gridded hydrometeorological dataset (German: hydrologische Rasterdaten)
MBCn		Multivariate Bias Correction method based on the n-dimensional probability density function transform (Cannon 2017)
obs		Observed values
P	mm	Precipitation
QDM		Quantile Delta Mapping (univariate bias correction method) (Cannon et al. 2015)
Q	mm	Streamflow
Q_I	mm	Simulated streamflow component resulting from glacier ice melt
Q_R	mm	Simulated streamflow component resulting directly from rainfall
Q_S	mm	Simulated streamflow component resulting from snowmelt
RCM		Regional Climate Model
RCP		Representative concentration pathway. RCP 4.5 and RCP 8.5 are different emission scenarios based on which the RCMs are run
ref		Reference data
sim		Simulated values
SLF		WSL Institute for Snow and Avalanche Research (German: WSL-Institut für Schnee- und Lawinenforschung)
SWE	mm	Snow water equivalent
T_a	°C	Air temperature

Abstract

Alpine catchments show a high sensitivity to climate due to their location within the elevation range of the snow line. Under these conditions around the melting point the interdependence of air temperature and precipitation are of major importance as they determine the physical state of precipitation which in turn influences the catchments' water balance. Especially water stored in the snow cover or glacier ice characterizes the catchments' runoff regimes. The correct representation of the climate input variables is therefore of major importance for hydrological simulations. For future simulations climate model data from the Euro-CORDEX ensemble were used for two emission scenarios (RCP 4.5 and 8.5). Before the climate data's use, systematic biases had to be corrected. The correction was done using a commonly applied univariate quantile mapping approach. In addition, as the interdependence of climate variables in alpine catchments is of proven relevance, a lately developed multivariate bias correction method was used that preserves the climate variables' interdependencies throughout the correction process. Remarkable differences were found in both, the variation of various regional climate models and the distinctions deriving from the two bias correction methods, especially for snow related processes. Moreover, changes evoked by changing climate were modelled until 2100 utilizing the semi-distributed HBV-light model. Glaciers were simulated to decrease or even vanish during the simulation period. Snow accumulation and the duration of snow cover were modelled to decrease as well. This will have considerable effects on the streamflow, as the catchments' nivo-glacial runoff regimes are mainly characterized by snow and glacier ice melt. This study was conducted in four partly glacierized mesoscale catchments in the Swiss Alps.

Zusammenfassung

Alpine Einzugsgebiete weisen aufgrund ihrer Lage auf Höhe der Schneegrenze eine ausgeprägte Klimasensitivität auf. Unter diesen Bedingungen, um den Schmelzpunkt, ist der Zusammenhang von Lufttemperatur und Niederschlag von besonderer Bedeutung, da er den physikalischen Zustand des Niederschlags bestimmt und dadurch den Wasserhaushalt in den Einzugsgebieten beeinflusst. Vor allem Wasser, das zunächst in einer Schneedecke oder in Gletschereis gespeichert wird, charakterisiert die Abflussregime der Einzugsgebiete. Die korrekte Darstellung von Klimavariablen als Modellinput ist daher von besonderer Relevanz für hydrologische Modellierungen. Für Zukunftsmodellierungen wurden Klimamodelldaten aus dem Euro-CORDEX Ensemble für die beiden Emissionsszenarien RCP 4.5 und RCP 8.5 verwendet. Bevor die Klimamodelldaten jedoch angewandt werden können, müssen systematische Verzerrungen korrigiert werden. Die Korrektur wurde mit einem weit verbreiteten, univariaten Quantile Mapping Ansatz durchgeführt. Da der kombinierte Effekt von Klimavariablen in alpinen Einzugsgebieten jedoch nachgewiesenermaßen von Bedeutung ist, wurde darüber hinaus noch eine kürzlich entwickelte, multivariate Korrekturmethode angewandt, die die gegenseitige Abhängigkeit von Klimavariablen während des Korrekturprozesses erhält. Vor allem für Schnee-bezogene Prozesse wurden bemerkenswerte Unterschiede gefunden, sowohl was die Variationen der verschiedenen regionalen Klimamodelle (RCMs), als auch die Unterschiede, die aus der Bias-Korrektur hervorgehen, betrifft. Des Weiteren wurden durch den Klimawandel hervorgerufene Veränderungen unter Verwendung des semi-distribuierten HBV-light Modells bis 2100 modelliert. Die Simulationen ergaben einen Rückgang und teils das Verschwinden von Gletschern, sowie eine Abnahme der Schneeakkumulation und der Dauer der Schneebedeckung. Dies hat erhebliche Auswirkungen auf den Abfluss, da die nivo-glazialen Abflussregime der Einzugsgebiete hauptsächlich von der Schnee- und Gletscherschmelze bestimmt werden. Diese Studie wurde in vier teilvergletscherten, mesoskaligen Einzugsgebieten in den Schweizer Alpen durchgeführt.

1 Introduction

1.1 Motivation

In times of changing climate, the Alps experience major changes in hydrological systems as a consequence (Gobiet et al. 2014). alpine catchments are especially sensitive to changing climate as the topography's elevation covers the zero-degree line during most of the year (Stahl et al. 2016). The zero-degree line does not only determine the physical state of precipitation, but also snowmelt and glacier ice melt. This relation shows the importance of the combined effect of precipitation and air temperature that determines the catchment's storage capacities and the water availability (Gobiet et al. 2014, Stahl et al. 2016). Nowadays, high altitudes in the Alps are still characterized by snow cover and the existence of glaciers (Pellicciotti et al. 2010). An upward shift of the zero-degree line, as it is projected, will lead to decreased snow accumulation and retreating glaciers. The decreasing trend in snow fall and accumulation as well as glacier wastage have already been observed within the last century and are expected to continue in the future (Huss & Fischer 2016). Catchments with a high fraction of melt water in runoff are likely to suffer from the lack of snow and glacier contribution possibly resulting in less water availability during often dry summer months. The decrease might affect both, groundwater recharge and surface runoff (Bavay et al. 2009).

The projected change in water availability, in turn, leads to socio-economic and ecological problems as streams represent an important lifeline for many European regions (Huss 2011). Water resource management needs to be adapted to less water availability during the summer - especially in dry inner alpine valleys. While groundwater levels might be sinking, irrigation might become limited. Furthermore, hydropower generation and shipping need to be adapted to the changing variability of water availability (Huss 2011). Moreover, winter tourism that currently dominates the economy in high elevated areas, relies on the presence of glacier remnants and snow accumulation (Schmucki et al. 2017). Additionally, the alpine biota is very sensitive to snow depth and the timing of snowmelt. Slight changes of these factors might therefore have serious consequences to the survival of rare, highly specified species (Schmucki et al. 2017).

To realistically assess changes in the water availability, hydrological models need to simulate the hydrological situation as accurate as possible. As the climate sensitivity is so high in the Swiss Alps (Stahl et al. 2016), a good representation of the climate variables as model input is obligatory. Simulating future conditions, climate variables are mostly derived from regional climate models (RCM). RCMs, however, often have systematic biases, that need to be corrected. Properly correcting these biases is a major challenge that needs to be addressed with caution. A special focus should be placed on preserving the multivariate interdependencies of relevant climate variables, as the combined effect of precipitation and air temperature is of major importance in highly elevated, glacierized catchments (Stahl et al. 2016).

1.2 Climatic and hydrological situation in the Swiss Alps

1.2.1 Climate and climate sensitivity

The central European climate is largely influenced by Westerly currents from the Atlantic Ocean delivering mild and humid air masses. Yet, the Alps represent an important North-South barrier dividing Europe and Switzerland in a Northern and Southern part. Especially during winter the influence of the Mediterranean Sea in the South leads to milder temperatures in comparison to the Northern parts. The temperature range in Switzerland is generally quite pronounced and primarily dependent on the altitude. High elevations have Arctic temperatures (annual mean temperature Jungfraujoch (3580 m a.s.l.): $\sim$ -7.5°C), while the Southern low-lands can enjoy rather Mediterranean temperatures (annual mean temperature Locarno/Monti (367 m a.s.l.): $\sim$ 11.5°C), generally 2-3 K higher than in the northern lowlands (annual mean temperature Basel (278 m a.s.l.): $\sim$ 10.0°C). Precipitation is spread throughout the year, while the amount of precipitation during the summer is nearly double to that in winter. As well as the temperature, precipitation is dependant on the topography. In the northern lowlands, the annual precipitation is around 1000-1500 mm/a. Along the northern foothills of the Alps, the average precipitation is around 2000 mm/a. However, in some rather dry valleys, well sheltered by surrounding mountains, annual precipitation does not exceed 500-700 mm (FOEN, 2014, HADES, 2010).

However, during the past 150 years the climate has changed. Higher air temperatures and increasing amounts of precipitation were registered throughout Switzerland (Hänggi & Weingartner 2011). Air temperatures have increased in yearly mean, and both minimum and maximum. However, the strongest signals of the increasing trend in air temperature was found during the summer month, whereas no trend could be detected for air temperatures in autumn. Especially during the last decades, an unusually high number of months with positive temperature anomalies was detected in comparison with the long-term annual mean (Scherrer et al. 2006). Precipitation and evaporation increased only slightly and not significantly (Hänggi & Weingartner 2011). Yet, as a result of increasing temperatures, the solid part of precipitation is decreasing and a shift from snowfall to rainfall was registered (Pellicciotti et al. 2010).

Catchments in the Swiss Alps are highly sensitive to the climate variables precipitation and air temperature and are therefore considerably influenced by the combination of the two (Stahl et al. 2016). Of major importance are snow fall and accumulation, which both are extremely sensitive to precipitation and air temperature. The temperature dependent shift of precipitation from rain to snowfall determines the storage and accumulation of snow. The winter precipitation amount determines the snow cover thickness (Schmucki et al. 2017, Jenicek et al. 2016). Furthermore, the snow and glacier melt are affected by air temperature. Air temperatures in spring determine the onset of snowmelt (Jenicek et al. 2016), whereas air temperatures during the summer affect the glacier melt rate. During the last decades since the

1980s snow and glacier melt rates changed significantly (Stahl et al. 2016). Climate sensitivity is of special importance in the elevation band between 1000 and 2500 m a.s.l., where the snow line shifts with the course of the year. These will also be the elevations most affected by climate change (Jenicek et al. 2016).

1.2.2 Climate projections based on regional climate models

In line with climate changes during the past century, a further increase in the mean air temperature is projected. In alpine regions, the strongest increase in air temperature is expected for the summer months (Köplin et al. 2010). Moreover, an increase in its year-to-year variability is assumed and the climate would become a little less stable (Hänggi & Weingartner 2011). Precipitation is projected to increase by 15-25% during autumn in the Northern alpine region. At the same time, a decrease of 15-25% in the mean precipitation during the summer months is expected in the Southern and Western part of Switzerland. This indicates a more or less stable annual precipitation amount (Köplin et al. 2010).

Climate projections mostly rely on the simulations of climate models. For climate change impact studies, mostly regional climate models are used, that simulate climate on a rather coarse continent-wide scale. The climate models are driven based on emission scenarios. These scenarios, such as the RCP (Representative Concentration Pathway) scenarios or the older SRES scenarios (Special Report on Emissions Scenarios) are based on economic data and include major goals of climate conferences (van Vuuren et al. 2011).

As topography and physical processes in global and regional climate models (GCM, RCM) are represented in a coarse and simplified way, modelled climate data often show some systematic biases of climate variables. A quite frequent problem is the 'drizzle effect', where too much precipitation is simulated on dry days (Maraun 2016). However, for climate change impact studies reliable input is obligatory, best, in a finer resolution than the one that can be modelled in RCMs. Therefore, modelled data need to be corrected and downscaled (Teutschbein 2010). This is done in a separate step based on a statistic relation without considering the physical background of the bias (Sippel et al. 2016).

Most bias correction methods can correct only one variable at a time (Vrac & Friedrichs 2014). These are univariate methods that are mostly simple and aim to correct mean values of distributions. However, there are more complex methods, that also preserve the distribution's standard variation or daily variability of different seasons that give the change to preserve trends in climate change, such as the correction of distribution functions or delta change corrections (Teutschbein 2010). The most commonly used univariate bias correction methods are based on correcting quantiles (Sippel et al. 2016). 'Quantile mapping bias correction algorithms have been reviewed in the context of hydrological impact studies and have been found to outperform simpler bias correction methods that correct only the mean or variance of precipitation series' (Cannon et al. 2015). For possible comparison with other studies and because of its often and widely accepted application, univariate quantile delta mapping (Cannon et al. 2015) is used in this project to correct the climate model data. This method allows keeping a climate change signal.

Recently, multivariate bias correction methods have been developed, that consider and preserve the dependence structure of climate variables such as precipitation and temperature. Due to the high climate sensitivity of runoff in Swiss catchments, the correct representation of the climate variable's interdependence is crucial to model snow accumulation or rain-on-snow events. One method is the empirical copula bias correction by Vrac & Friedrichs (2014). After applying a regular univariate bias correction, the data is resorted based on the Schaake shuffle introduced by Clark et al. (2004). However, the ranking structure needs observed data for the same time-period and cannot be applied on future projections (Vrac & Friedrichs 2014). Mehrotra & Sharma (2016) developed a multivariate recursive quantile nesting bias correction that can be applied for correcting future projections as well. It is a complex combination of equidistant quantile mapping by Li et al. (2010), persistence-based nesting bias correction as developed by Johnson & Sharma (2012) and recursive logic by Mehrotra & Sharma (2012). Time series are corrected to match the observed data in auto- and cross correlation. Another multivariate bias correction method is the multivariate extension of linear rescaling with a Cholesky decomposition introduced by Bürger et al. (2011). It preserves both, mean and variance of a data distribution as well as the dependence structure of the variables. However, it is lacking a correction of the marginal distribution. To additionaly correct the marginal distribution, Cannon (2016*b*) developed an approach combining the method by Bürger et al. (2011) with univariate quantile mapping, in order to correct the data's marginal distribution. Depending on the data's distribution, Cannon (2016*b*) proposes variants based on the Pearson correlation or the Spearman rank correlation.

The latest development by Cannon (2017) is based on the N-dimensional probability density function transform (N-pdft). The approach was originally developed for image processing, but converted to be used to process climate model data. The multivatiate bias correction (MBCn) method uses a combination of QDM and the N-dimensional density probability transform to match the multivariate distributions of climate model data and observed data. QDM corrects the marginal distributions of the data while including a rotation of the data points by 90° and therefore introducing a linear combination preserves the interdependence of the climate variables. The rotation is applied before QDM and the data is rotated back after the bias correction. These steps are conducted iteratively until the multivariate distributions of model data and observed data match.

1.2.3 Snow and ice cover

The snow cover is highly sensitive to the climate variables precipitation and temperature and therefore heavily affected by climate change (Bavay et al. 2009). However, in comparison to the strong increase in air temperature, the relatively small increase in winter precipitation has almost no effect on the observed and projected decrease in snow cover (Zubler et al. 2014, Schmucki et al. 2017). The temperature dependent decrease of the solid fraction of precipitation and the extension of snowmelt lead to a reduced number of days with snowfall, a reduce in the mean snow depth and a shorter duration of snow cover (Pellicciotti et al. 2010). While under the current climate conditions permanent snow and ice cover is still possible above 3000 m a.s.l.,

the zone would disappear under predicted climate conditions (Bavay et al. 2009). According to Bavay et al. (2009), characteristic zones of snow cover would be shifted upward by around 900 m by the end of the 21^{st} century. A continuous snow cover during the winter would be likely to exist only in altitudes above 2000 m a.s.l.. In mid elevations (1000-1700 m a.s.l.) snow cover would be interrupted and of shorter duration. Below 1000 m a.s.l. continuous snow covers would become rare, while below 500 m even snowfall would become an exception with possibly only two days per year. For these low elevations the strongest relative reduction of about 90% of the mean snow depth during winter is projected (Schmucki et al. 2017).

As well as snow accumulation, fluctuations of mountain glaciers are sensitive to the climate variables air temperature and precipitation and therefore changing climate (IPCC 2013, Fischer et al. 2015). Since the maximum extent of alpine glaciers during the Little Ice Age in the mid-19^{th}-century, glaciers all over the European Alps were showing mass losses (Zemp et al. 2008). Apart from short periods of stagnation or slightly positive mass balances at the end of the 19^{th} century, during the late 1910s and from the late 1970s to the mid-1980s, glaciers were generally retreating: A trend, that accelerated in the 1980s (Glaciological Reports 1958/59-2010/11). Between 1980 and 2010, Swiss glaciers lost around -22.51 $\pm$1.76 km^3 of volume (Fischer et al. 2015). While in 1973, 1261.2 km^2 were covered by glaciers in Switzerland, which is equivalent to 3.89% of the country's total area, in 2010, only 942.8 km^2 were still covered by glaciers, which equals 3.04% of Switzerland's total area (Fischer et al. 2015). Especially very small glaciers react comparatively quickly to temperature changes and are therefore highly vulnerable to climate change. Prominent mass losses and glacier wastage have been observed over the last century. Since the 1970s, the total of very small Swiss glaciers has declined by 50-75%, losing up to 70% of their previous area. Many very small glaciers have already disappeared throughout the past century (Huss & Fischer 2016). Glacier volume changes were observed to be greatest at the elevation band between 2700 and 2800 m a.s.l.. Yet, they were noticeable even above 3500 m a.s.l.. From the 1980s onward, no elevation band showed positive glacier mass balances (Fischer et al. 2015).

For the future, a further decline in both, glacier thickness and area are expected. Until 2040 around 50% of very small glaciers in Switzerland are projected to vanish. By 2060, 97% of all very small glaciers (< 0.1 km^2) have likely disappeared assuming the A1B-scenario. Of the size class from 0.1-0.5 km^2 88% of the glaciers are projected to be gone by 2060, 11% by 2030. In a similar manner, glacier wastage is simulated for other size classes as well (Huss et al. 2008). However, glacier retreat is a slow process and mass losses are limited (Huss & Fischer 2016).

While gently sloping, debris-covered glaciers at low elevation are most sensitive to rising air temperatures, some glaciers react less sensitive to these changes and might survive until the end of the 21^{st} century. At very high elevations glaciers might stop frontal mass loss after retreating from the break-off ledge. In addition, some glaciers - even at lower elevations - are protected from solar radiation in niches and cirques below north exposed rock walls. Often, extreme accumulation of snow through high precipitation, wind drift or avalanches can be observed in cirques feeding the glacier. Generally, a large thickness to length ratio slows down the glacier melting process (Huss & Fischer 2016).

1.2.4 Runoff and its components

Runoff regimes in Switzerland are dependent on the catchment's region, elevation and glacierization. For many catchments, storage of precipitation in the form of snow or ice is determining the runoff. While precipitation is stored in snow cover during the winter, very little runoff is observed. During snow or glacier melt in spring and summer, runoff peaks will be reached in alpine rivers. Therefore, regimes are characterized as nival or glacial. Exemplary, the nivo-glacial regime of the Weisse Lütschine is shown in Figure 1.1. However, in the Swiss lowlands, precipitation runs off mainly directly and some runoff regimes can be characterized as partly pluvial (Blanc & Schädler 2013).

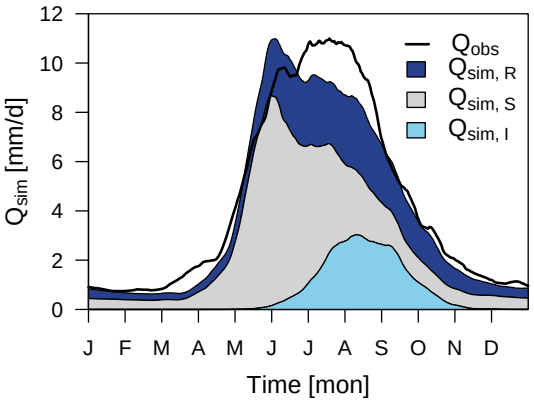

Figure 1.1: Nivo-glacial runoff regime. Exemplary shown is the streamflow data of the Weisse Lütschine aggregated over the 30-year period from 1977-2006. Data according to Stahl et al. (2016).

In partly glacierized catchments runoff is highly sensitive to air temperature. In elevations above 1500-2000 m a.s.l. temperature sensitivity is dominant during spring and summer. Due to snowmelt and glacier melt later during the summer, temperature sensitivity stays positive throughout the summer and significant until October - in the highest regions above 2500 m a.s.l. even until early November. During the winter, temperature sensitivity is low, as precipitation is stored and accumulated in snow not directly contributing to runoff. However, temperature sensitivity turns slightly positive during the winter with decreasing elevation. Under the assumption of lacking glacierization in the future, temperature sensitivity of runoff during the summer will be decreasing and shifting further to higher elevations (Stahl et al. 2016).

In mean elevations above 2000 m a.s.l., precipitation sensitivity is rather low from November through May. In largely glacierized and high catchments, no precipitation sensitivity could be detected in January. This effect is due to the increasing probability of snow cover with altitude: As precipitation is stored in the snow cover, it is irrelevant for direct runoff. However, from May onward during the summer, precipitation sensitivity becomes more pronounced until the end of October. The solid part of precipitation is decreasing during the summer, and liquid precipitation can directly influence the streamflow. Below 1000-1500 m a.s.l. precipitation sensitivity is positive and dominant for runoff during the winter. Under the assumption of decreasing glacierization, precipitation sensitivity to runoff will increase (Stahl et al. 2016).

Snow cover, accumulated during winter, causes runoff peaks in spring or early summer. There is a significant contribution of snowmelt to runoff from May until middle or late summer in September. In lower elevation catchments, the influence

of snowmelt is limited to June and July, while in higher catchments, snowmelt contributes most during July and August. In catchments above 2000 m a.s.l. the effect of snowmelt is decreasing and occurring only in August and September (Jenicek et al. 2016). The amount of snow accumulated is also associated with the long-term mean streamflow. The more snow has accumulated during winter, the longer melting snow can affect low flows during the subsequent summer. Furthermore, snow covers affect groundwater recharge, likewise contributing to runoff during the summer season. In some high-elevation areas in the Swiss Alps, for example, the effects of the 2003 summer drought were mitigated by above average snow resources that contributed to the streamflows (Zappa & Kan 2007). The sensitivity of summer low flow to snow accumulation increases with the mean catchment elevation (Jenicek et al. 2016). Furthermore, the snow cover in its amount and duration has an impact on glaciers and their runoff. The snow contributes through its accumulation during the winter directly to the glacier mass balance as well as indirectly, by affecting the timing of the ice melt onset (Pellicciotti et al. 2010). Under projected future climate conditions, changes in snow cover affect both, the characterisation and the timing of river discharge in alpine catchments (Bavay et al. 2009). With less snow accumulation during winters, less melt water will be available in spring (Hänggi & Weingartner 2011). Higher temperatures would melt the snow earlier and quicker, causing a narrower and earlier peak of discharge in spring (Bavay et al. 2009). The reduction in snow water equivalent and the earlier onset of snowmelt are likely to result in earlier low-flow occurrence during the summer. Especially catchments at mid- and high elevations are likely to become more sensitive to meteorological droughts (Jenicek et al. 2016).

The observed glacier wastage due to increasing air temperature affects the streamflow. The higher energy receipt and feedback mechanisms such as a decreasing albedo, caused by lacking snow, lead to increasing glacier ice melt and increased streamflow, which is especially visible in highly glacierized catchments (Pellicciotti et al. 2010). Parallel to this process, glacier area is reduced considerably, which diminishes streamflow. Runoff trend analyses show evidence for both processes (Pellicciotti et al. 2010). In total, they could so far level each other, so that no trends could be observed in the Swiss Alps. However a glacier runoff peak is expected, after which the glacier area becomes too small to even out the reduction of the glacier size (Stahl et al. 2016). For several Swiss catchments, the runoff peak is projected to be reached between 2020 and 2050. Until then, larger glaciers will still be able to compensate their mass loss. For smaller glaciers the maximum glacier contribution was already reached between 1997 and 2004. Their water release is therefore already declining. In general, specific glacier runoff in August and September will be reduced and by the end of the 21^{st} century, when currently glacierized catchments might contribute 55-85% less water to streamflow discharge (Huss 2011).

Based on its heritage directly from precipitation or indirectly from different storages, runoff parts can be separated. The streamflow that does not derive directly from precipitation is dependent on the capacities and characteristics of the storages, that might be the snow cover, glaciers, soil, ground water or surface water such as lakes. Apart from the inter-annual variability in runoff parts, there is a high variability from year to year and long-term trends are barely recognized (Stahl et al. 2016).

In Swiss glacierized catchments, the runoff part of snowmelt is dominant during April and Mai, which is then followed by the ice melt of glaciers. During the winter, the importance of these runoff components diminishes. At the gauge of the Rhine River in Basel, 59% of the runoff between June and August derives from snowmelt, and 8% from ice melt. If the period is extended until September the snowmelt part of the runoff decreases to 47% while the ice melt part increases to 10%. The part of glacier melt water is generally small in the context of the entire water balance, but - especially during low flow periods in the summer - of high importance. The highest amount of absolute glacier melt water drains in August. The highest relative part is reached during September and October, when the influence of snowmelt becomes non-relevant (Stahl et al. 2016). Even further downstream in large catchments, ice melt water can be a significant component of streamflow runoff, especially during low flows the ice melt season within the summer months (Huss 2011). Reduced glacier volumes will therefore lead to a noticeable decrease in runoff during the late summer. Huss & Fischer (2016) projects a reduction in runoff from glacierized catchments in August of more than 60% by 2060, compared to the mean August runoff from 1961-1990.

As the snow and glacier melt induced runoff components change, the total streamflow changes. From 1900-2000 mean summer runoff in Switzerland decreased slightly, while the mean winter and spring runoff increased significantly due to milder winters, in which less precipitation is stored as snow and therefore contributes directly to runoff (Stahl et al. 2016). This signifies a decreasing intra-annual variability during the last two centuries. Furthermore, the mean annual runoff was quite stable within the 20^{th} century and did not change significantly (Hänggi & Weingartner 2011). As air temperatures are projected to increase further in the future, more runoff is projected to be generated during autumn and winter, while it is likely to diminish in summer. Heavy precipitation events in autumn would change from mainly solid to mainly liquid precipitation and would be more likely to produce flooding (Bavay et al. 2009). During winter there is a positive trend in the runoff component deriving directly from precipitation. The decreasing spring and summer runoff will be owed to less accumulated snow and diminishing glaciers to melt along with an earlier stop of the snowmelt. However, the total annual runoff might only show a slightly positive trend, if any (Stahl et al. 2016). Likewise behaves the year-to-year variability, that is not expected to change significantly (Hänggi & Weingartner 2011).

1.2.5 Research gap

Within the last years, many studies have done assessments of the impacts of the changing climate in the Swiss Alps focussing on hydrological systems. While some studies simulate runoff on macro-scale catchments (Rhine, Rhone, Po, Danube) (Huss 2011), often, only individual parts of the hydrological system, such as glaciers, snow accumulation or runoff are assessed (Pellicciotti et al. 2010, Fischer et al. 2015, Huss et al. 2008). Not many studies consider different components of the hydrological system and track them even in the streamflow. In the ASG-project (Stahl et al. 2016), all necessary components of the water balance in the Rhine catchment area were simulated using the HBV-model. This allowed tracking the streamflow's origin from

rainfall, snowmelt or glacier ice melt and easily detecting changes in the long-term trends in the runoff components themselves, even though the total runoff remained rather stable during the entire simulated time period. However, simulations were conducted based on (partly reconstructed) observation data for the 20^{th} century. The field, that is still open, is the assessment of snow cover, glacier volume and runoff trends including its components in future time periods.

Simulating prospective periods mostly implies the use of representative climate model (RCM) data. To receive these, biases in the RCM output data need to be corrected as argued before (subchapter 1.2.2). So far, most climate change impact studies use univariate bias correction methods such as quantile mapping to correct biases in the climate model output. As climate sensitivity and especially the interaction of the climate variables precipitation and air temperature are of major importance in alpine catchments, the climate variable's interactions should be considered and as far as possible preserved while correcting. Within the past five years, a relatively new field of multivariate bias correction techniques has been explored and developed. Still, not many studies consider the climate variable's interactions by applying the lately developed bias correction techniques.

1.3 Objectives

The aim of this study was to simulate runoff and its components from four glacierized mesoscale catchments in the Swiss Alps under future climate conditions. Therefore, the ASG-project's (Stahl et al. 2016) modelling approach was applied for future time periods and snow accumulation and glacier volume as well as the catchment's runoff and its components were simulated. The research question was to assess the influences of the changing climate on future snow cover and glacier volume. Furthermore, the combined effect of these components on the catchment's streamflow regime was evaluated.

Another objective of this study was to take the opportunity that the lately developed multivariate bias correction methods provide and correct the regional climate model's output preserving the climate variable's interactions. The multivariate corrected climate model output and its transfer in hydrological modelling will be compared with results using the so far standard univariate quantile mapping. Differences and common features of the two correction approaches are assessed in relation to the general variability of an RCM ensemble from the Euro-CORDEX dataset as well as their impact on hydrological simulations.

2 Methodology

2.1 Study area

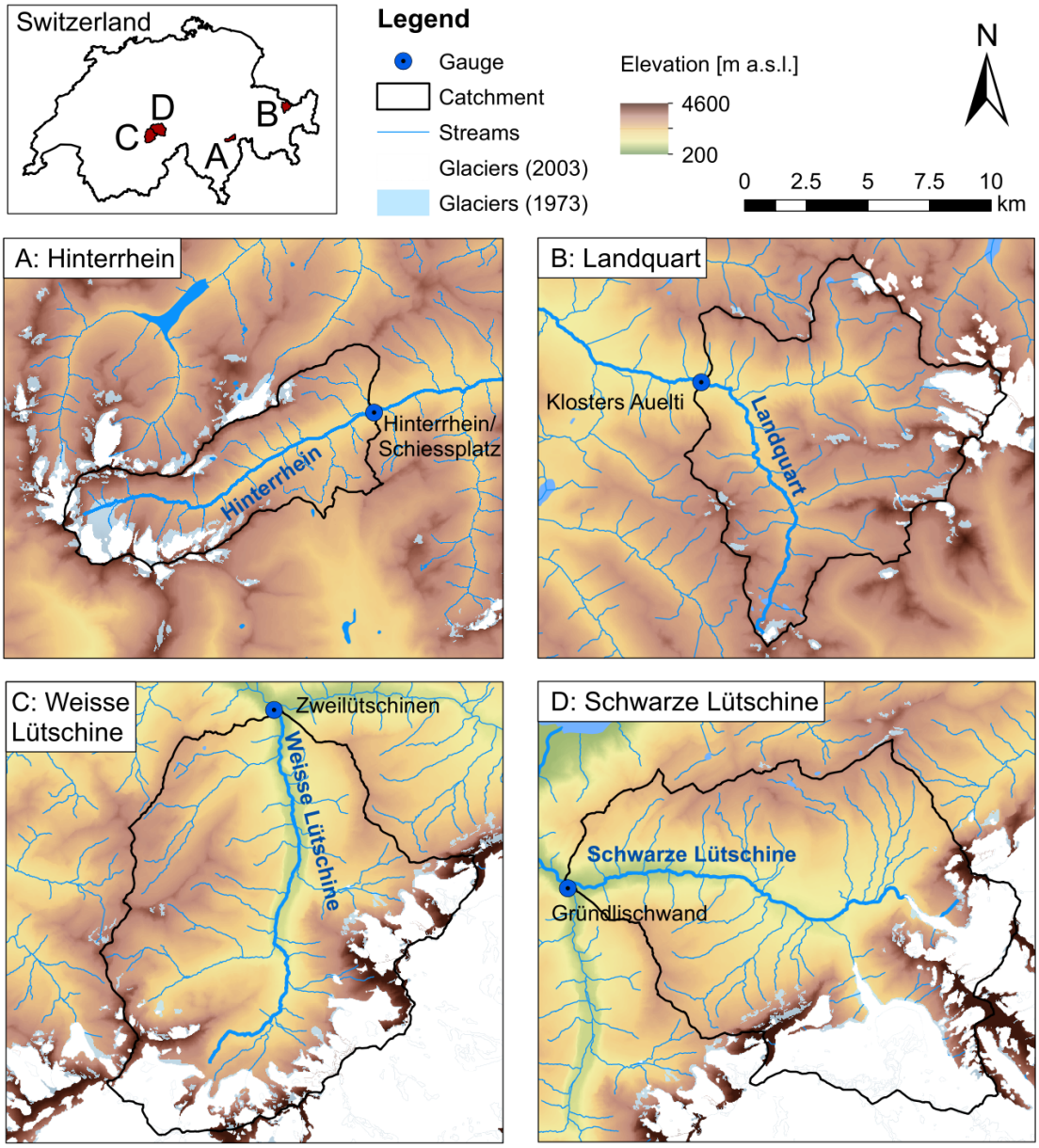

Figure 2.1: The four evaluated Swiss catchments: Hinterrhein (A), Landquart (B), Weisse Lütschine (C), Schwarze Lütschine (D). The glacierized area in 1973 is displayed in light blue, the glacierized area in 2003 in white.

As shown in the map in Figure 2.1, the study area includes four catchments influenced by glaciers in the Swiss Alps in the Rhine catchment area. One of them is the Hinterrhein catchment (Fig. 2.1 A) in Graubünden, the smallest of the evaluated catchments with a size of 53.9 km^2 and a comparatively small elevation range of 1800

m around a mean elevation of about 2350 m a.s.l.. The glacier extent has decreased between 1900 and 2010 from formerly 17.1 km^2 to just 3.8 km^2 in 2010, which is equivalent to a glacier covered area of formerly almost 18% to just 7% in 2010. One of the larger firn basins in the area is the Rheinwaldfirn, that feeds the Paradies and the Zapport glaciers (HADES, 2010, Tafel 3.1). The Landquart catchment (Fig. 2.1 B) is about twice the size, measuring 103 km^2. The mean elevation and the elevation range are similar to the Hinterrhein catchment. The glacierized area decreased from 12.4 km^2 in 1900 by two thirds to 4.4 km^2 in 2010, which is equal to 8% and a little more than 4% of the catchment area. The catchment is situated in Graubünden as well including glaciers of the Verstankla group and the Silvretta group (HADES, 2010, Tafel 3.1). The last two catchment areas are the ones of the two headstreams of the Lütschine in the Berner Oberland discharging into the Aare. The Schwarze (Fig. 2.1 D) and Weisse Lütschine (Fig. 2.1 C) catchments are 180 km^2 in size and 165 km^2 respectively and include some of the highest mountains in the European Alps such as Jungfrau (4158 m), Mönch (4099 m) or Eiger (3970 m) (HADES, 2010, Tafel 1.1). Accordingly, glacierization is higher in comparison to the first two catchments decribed. In 2010, 30 km^2 (17%) were glacierized in the Schwarze Lütschine catchment area and 21.4 km^2 (13%) in the Weisse Lütschine catchment area, with an in relative means smaller glacier decrease compared to the other two catchments. The catchments also hold some of the largest Swiss glaciers such as the Grindelwald glaciers in the Schwarze Lütschine catchment area or the Breithorn glacier in the Weisse Lütschine catchment area (HADES, 2010, Tafel 3.1). The characteristics of the four evaluated catchments are listed in table 2.1.

2.2 Data and data preparation

Historic observation data were used for the model calibration. Among those were streamflow data, meteorological data, snow water equivalent (SWE) and snow cover data and estimates of glacier area and volume as presented in Figure 2.2.

The streamflow data used for the HBV-light calibration for the four main gauges were measured by the Swiss Federal Office for the Environment (FOEN). Runoff data were available for the entire calibration period and warm-up time (1973-2006) for three of the catchments: Hinterrhein (gauge: Hinterrhein), Schwarze Lütschine (gauges: Gsteig-Zweilütschinen, Gründlischwand only available for limited years) and Weisse Lütschine (gauge: Zweilütschinen). For Landquart runoff was measured at the gauge Klosters Auelti until 2004.

As meteorological reference data, the HYRAS raster data set (1951-2006) was used. It is a product by the German Weather Service (DWD) and the German Federal Institute of Hydrology (BfG) providing interpolated air temperature and precipitation data at a grid size of 1 km^2. However, it was shown by Stahl et al. (2016) that precipitation is significantly underestimated in the alpine catchments and therefore corrections were necessary. In the ASG-project (Stahl et al. 2016) data was corrected referring to a raster based application by Sevruk (1989) to correct precipitation in dependency of wind correction and compared to the hydrological atlas HADES, 2010. In case of large differences, a second correction step was ap-

Table 2.1: Catchment characteristics. Data were taken from Stahl et al. (2016). Glacier volume was calculated based on the literature in brackets.

Catchment	Hinterrhein	Landquart	Schwarze Lütschine	Weisse Lütschine
Size [km^2]	53.9	103.0	179.9	164.9
Elevation [m.a.s.l.]				
Mean elevation	2357	2339	2059	2149
Min. elevation	1587	1321	648	650
Max. elevation	3387	3296	4086	4146
Elevation range	1800	1975	3438	3496
Glacier volume [km^3]				
1973 (Huss et al. 2010)	0.31	0.28	1.99	1.13
2003 (Paul et al. 2011)	0.13	0.18	1.08	1.07
2010 (Huss et al. 2010)	0.10	0.18	1.60	0.85
2010 (Fischer et al. 2014)	0.10	0.16	1.54	0.81
Glacier extent [km^2] ([%])				
1973	9.1 (17.82)	7.9 (7.74)	37.0 (23.53)	28.8 (18.48)
2003	4.7 (8.72)	4.9 (4.76)	34.4 (19.12)	26.3 (15.95)
2010	3.8 (7.05)	4.4 (4.27)	29.7 (16.5)	21.4 (12.98)

plied using area specific correction factors based on the water balance as described by Weingartner & Schädler (2001) in HADES, 2010, Tafel 6.3. Especially the precipitation in Landquart had to be increased by further 50%. SWE and snow cover data were derived from empirical maps by the Institute for Snow and Avalanche Research (SLF). The glacier area was assessed based on aerial and satellite photographs by Müller et al. (1976) (1973), Paul et al. (2011) (2003) and Fischer et al. (2014) (2010). Based on these, the glacier volume was calculated using simulations by Huss (1973, 2010) and Volume-Area-Scaling (2003, 2010). In this study, the data as they were corrected and used in the ASG-project were adopted as basis for the model calibration and the bias correction of the climate model data.

For HBV-light simulations potential evapotranspiration as well as temperature lapse rates and precipitation gradients had to be determined. Based on the corrected HYRAS data, evapotranspiration was calculated using a temperature based method according to Oudin et al. (2005). The 11-day moving average (rough duration of marco weather situations) of the mean daily evapotranspiration values aggregated yearly from 1973-2006 was used throughout simulations. In highly elevated catchments evapotranspiration is no major factor in the water balance, so this estimation is sufficient. Furthermore, temperature lapse rates and the precipitation gradient were extracted from the corrected HYRAS dataset. For the temperature lapse rate, the 11-day moving average of daily annually aggregated data was used throughout simulations. As precipitation gradient the mean of all daily values throughout the

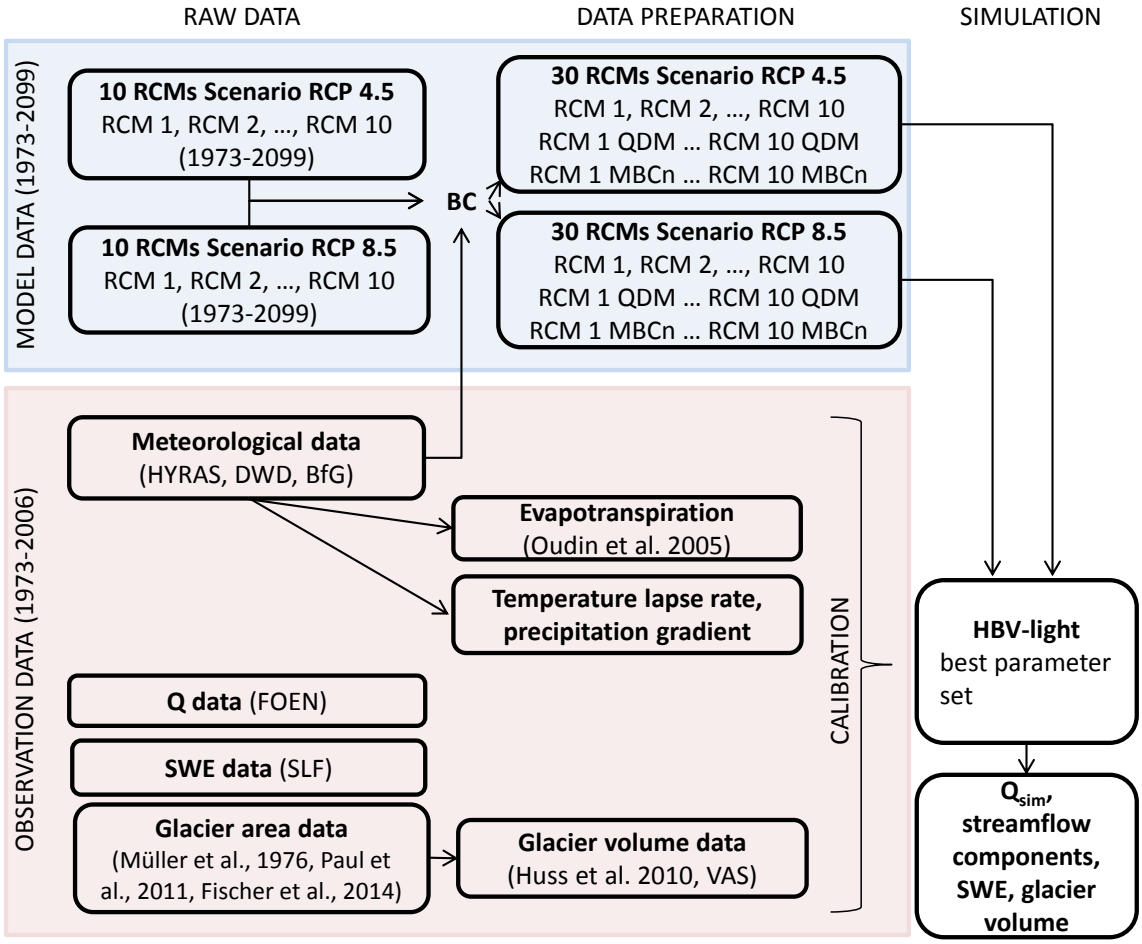

Figure 2.2: Schema of the available raw data of both, regional climate model data and observation data, as well as corrected and calculated data based on the raw data as preparation for the HBV-light calibration and simulation.

available time period was determined.

To simulate the runoff, climate model data from the European branch of the **Co**ordinated **R**egional Climate **D**ownscaling **Ex**periment (EURO-CORDEX) were used. The international CORDEX was initiated by the **W**orld **C**limate **R**esearch **P**rogram (WCRP) in order to collect and provide an improved dataset of regional climate change projections for land regions world wide. The improvement to the previous PRUDENCE and ENSEMBLE datasets is the finer grid resolution of 0,11°*0,11° and the inclusion of the updated greenhouse gas emission scenario simulations for the 21^{st} century. The CORDEX dataset provides the basis of climate change impact and adaptation studies within the fifth Assessment Report (CMIP5) of the **I**ntergovernmental **P**anel on **C**limate **C**hange (IPCC) and is considered the current standard in climate prediction (WCRP, 2015). Ten Regional Climate Models (RCMs) were examined from 1970-2100. One model (No. 8, RCA 4) does not consider leap years, however, all leap days were filled with the interpolated value of the previous and following day. All RCMs are listed in table 2.2.

Two scenarios were used to drive the RCMs in the EURO-CORDEX project:

RCP 4.5 and RCP 8.5. The **R**epresentative **C**oncentration **P**athways (RCPs) were also developed for the Fifth Assessment Report of IPCC (2013) and provide possible atmospheric compositions for the future. They are based on historical greenhouse gas concentrations, multi-gas emission scenarios, radiative forcing and agricultural land use. Referring to pre-industrial levels, the RCP 8.5 assumes a rising radiative forcing pathway reaching 8.5 W/m^2 ($\sim$ 1370 ppm CO_2 eq) by 2100 and represents the upper end of the possible range with the highest baseline of greenhouse gas emissions according to current literature. RCP 4.5 is an intermediate scenario and will stabilize at a radiative forcing of 4.5 W/m^2 ($\sim$ 650 ppm CO_2 eq.) which is simulated to be reached towards the middle of the 21^{st} century (Meinshausen et al. 2011, van Vuuren et al. 2011).

Table 2.2: RCMs from the Euro-CORDEX data set used in this project.

No.	Institution	Driving GCM	RCM
1	CLM Community	CNRM-CM5-LR	CCLM4-8-17
2	Swedish Meteorol. & Hydrolog. Institute	CNRM-CM5	RCA4
3	CLM Community	EC-EARTH	CCLM4-8-17
4	Danish Meteorological Institute	EC-EARTH	HIRHAM5
5	Royal Netherlands Meteorol. Institute	EC-EARTH	RACMO22E
6	Swedish Meteorol. & Hydrolog. Institute	EC-EARTH	RCA4
7	Laboratoire des Sciences du Climat et de l'Environnement	IPSL-CM5A-MR	WRF331F
8	Swedish Meteorol. & Hydrolog. Institute	IPSL-CM5A-MR	RCA4
9	CLM Community	MPI-ESM-LR	CCLM4-8-17
10	Swedish Meteorol. & Hydrolog. Institute	MPI-ESM-LR	RCA4

2.3 Bias-Correction

For possible comparison with other studies and because of its often and widely accepted application, univariate quantile delta mapping (QDM) was used in this project to correct the climate model data. QDM is a quantile mapping approach by Cannon et al. (2015), that was designed to maintain trends in climate model data throughout the bias correction process. Therefore, the climate change signal (Δ) is extracted from all projected future quantiles in a first step (eq. 2). The quantile mapping is then applied to the detrended series, before the projected trend is reintroduced to the bias corrected model output (eq. 4). Quantile Mapping is based on a transfer function that transforms the cumulative distributions of the modelled towards the observed series. For each quantile with a nonexceedance probability (τ) of the historic time period the equivalent is searched in the observed time series, which gives the data's transfer function (eq. 1). The ascertained transfer function is then applied to all model data, to both time periods, historic and projected (eq. 3). In this study, univariate Quantile Delta Mapping was chosen because it corrects systematic dis-

tributional biases relative to historical observations and preserves model-projected relative changes.

$$\tau_{sim,p}(t) = F^{(t)}_{sim,p}[x_{sim,p}(t)], \tau_{sim,p}(t) \in \{0,1\} \tag{1}$$

$$\Delta_{sim}(t) = \frac{F^{(t)-1}_{sim,p}[\tau_{sim,p}(t)]}{F^{-1}_{sim,h}[\tau_{sim,p}(t)]} \tag{2}$$

$$\hat{x}_{obs:sim,h:p}(t) = F^{-1}_{obs,h}[\tau_{sim,p}(t)] \tag{3}$$

$$\hat{x}_{sim,p}(t) = \hat{x}_{obs:sim,h:p}(t)\Delta_{sim}(t) \tag{4}$$

τ	nonexceedance probability
t	time
F	cumulative distribution function
F^{-1}	inverse cumulated distribution function
x	time series of climate variable
$\hat{x}$	corrected series
Δ	relative change in quantiles
$_{sim}$	simulated
$_{p}$	projected
$_{obs}$	observed
$_{h}$	historical

The latest development by Cannon (2017) is a multivariate bias correction algorithm based on the N-dimensional probability density function transform (N-pdft). The approach was originally developed for image processing, but converted to be used to process climate model data. The multivariate bias correction (MBCn) method uses a combination of QDM and the N-dimensional density probability transform to match the multivariate distributions of climate model data and observed data. QDM corrects the marginal distributions of the data while including a rotation of the data points by 90° and therefore introducing a linear combination preserves the interdependence of the climate variables. The rotation is applied before QDM (eq. 5) and the QDM corrected dataset ($\hat{X}$) is rotated back afterwards (eq. 6). These steps are conducted iteratively until the multivariate distributions of model data and observed data match. In this case, 100 iterations were conducted.

$$\tilde{X}^j = X^j * R^j \tag{5}$$

$$X^{j+1} = \hat{X}^j * R^{j^{-1}} \tag{6}$$

X	matrix of climate variables
$\tilde{X}$	rotated matrix of climate variables
$\hat{X}$	QDM corrected matrix of climate variables
R	rotation matrix

Often, data is downscaled, while its bias is corrected. This is due to the often finer resolution of reference data in comparison to the coarse grid resolution of RCMs. In the case of this study, the reference HYRAS dataset has a grid resolution of 1 km^2, while the RCM data has a grid size of roughly 120-130 km^2, which is about catchment size of the study catchments. Especially for interpolations that are based on spatial resolutions, that differ substantially, problems can occur. One example would be local, orographic precipitation that through the interpolation is spread wider and overestimated (Cannon 2017). However, as there is no other option in the case of this study, than accepting possible biases to stay in the data, it is assumed that especially the MBCn method performs well enough.

2.4 HBV-light setup and simulation

To simulate runoff under modelled climate conditions, the HBV-light model (Hydrologiska Byråns Vattenbalansavdelnin) was used. It was originally developed by Sten Bergström at the Swedish Meteorological and Hydrological Institute (SMHI) in the 1970s for use in Scandinavia, but was meanwhile successfully applied in more than 30 countries, including Switzerland (Seibert & Vis 2012). The HBV-light model is a semi-distributed conceptual model. 'Semi' means, that different categories such as elevation classes or vegetation zones can be represented. 'Distributed' implies that the model can be based on raster data in contrast to lumped models, that consider catchment characteristics to be uniform (Seibert & Vis 2012). HBV-light can be used to simulate runoff data series, to investigate the effect of changes within the water balance or the catchment and to simulate effects of climate change (Seibert & Vis 2012). Furthermore, it allows to track the different components of streamflow such as components from rainfall, snowmelt or glacier ice melt. In the ASG-project (Stahl et al. 2016), the model was used for the same purpose of climate change influences on the streamflow of the river Rhine considering the long-term average streamflow components in the same glacierized, alpine catchments as evaluated in this study and led to consistent results.

The HBV-light model structure is based on the catchment's water balance, using data for precipitation (P), temperature (T) and potential evapotranspiration (ET_{pot}) as input to simulate daily runoff (Q_{sim}). Therefore different connected routines are implemented in the model to simulate the discharge. The model structure can be varied or adapted according to catchment characteristics. As shown in Figure 2.3, implemented routines are the snow routine, the soil moisture and evaporation routine, the response function, the routing routine and if needed, the glacier routine can be added (Seibert & Vis 2012).

Precipitation and temperature are assigned gradients according to altitude, if different elevation zones are used in the modelled catchment. The gradients are either calculated by the model using the parameters PCALT [%/100m] and TCALT [°C/100m] or given as additional input file (PTCALT). The precipitation in the model is separated into rain or snow based on a defined threshold temperature (T_T [°C]). If the temperature falls below the threshold temperature, the **snow routine** is used. After applying a snow fall correction factor (SFCF), to compensate for

systematic errors in measurements and sublimation from the snow cover, snow is accumulated. As soon as temperatures rise, snowmelt is calculated according to the degree-day method. The degree-day method is implemented using a seasonally varying factor (SP) for snowmelt as described in Stahl et al. (2008). Until the maximum water hold capacity (C_{WH} [-]) of the snow pack is reached, melt water and rainfall are retained and refrozen (refreezing coefficient C_{FR}), if temperatures drop below the threshold temperature (Seibert & Vis 2012). In this study, the three parameters C_{WH}, C_{FR} and SP were predefined.

Differences in snow accumulation originating, among others, from snow transport by avalanches or wind drift need to be considered, as it might lead to unrealistic snow accumulation at high elevations and as the spatial distribution of snow has an effect on the timing and amount of snowmelt runoff (Freudiger et al. 2017). The snow redistribution is conceptually implemented in the snow redistribution routine that was added to HBV-light for the ASG-project (Stahl et al. 2016) and will be used in this study. For the simulated catchments in this study, as well as in Stahl et al. (2016), snow was redistributed to lower areas or shifted to glacierized areas if more than 500 mm snow water equivalent (SWE) were accumulated in non-glacierized elevations above 2500-2700 m a.s.l.

The snowmelt water as well as the precipitation fallen as rain are transferred to the **soil moisture and evaporation routine**. Depending on the soil water content, the water will be distributed to actual evaporation (ET_{act}) that is calculated based on the potential evapotranspiration, or transferred to the **response function** as groundwater recharge. The response function simulates the groundwater volume and some variations of the model structure are implemented in the HBV-light model. The standard version includes two groundwater storages: an upper (SUZ) and a lower saturation zone (SLZ). Through percolation (PERC) from the upper to the lower zone the zones are connected, but release water independently. The outflow from the groundwater storages are simulated using recession coefficients (K_1, K_2). The drainage of the lower saturation zone represents the baseflow of the modelled catchment. Further options of the response routine structure include options with three groundwater boxes. The outflow out of the groundwater box equals the sum of the outflow of the different groundwater boxes (Seibert & Vis 2012). In the following **routing routine**, the discharge of the groundwater box and the glacier ice meltwater is transformed by a triangular weighting function including the delaying factor MAXBAS to yield the simulated runoff (Seibert & Vis 2012). Additionally, a **glacier routine** can be added (Seibert et al. 2017). It incorporates the Δh-parametrization by Huss et al. (2010) to simulate the glacier volume being based on an empirical approximation designed for periods dominated by negative mass balances and glacier retreat. Based on the glacier size, a type-curve empirically determined by Huss et al. (2010) will be chosen that allows to adapt glacier volume and area during the melting process. In the model the translation of glacier mass balance changes into area changes is represented in a lookup table, that allows the simulation of the glacier area to advance as far as the initial glacier area extent (Seibert et al. 2017). Each year, a small percentage (KSI) of the simulated snow cover is transformed to glacier ice. The glacier ice melt is also computed using the degree-day approach and the meltwater is added to the glacier's water content, from

which the outflow is computed according to Stahl et al. (2008) (Seibert et al. 2017). The temperature based, seasonally changing outflow from the glacier is added to the simulated runoff (Stahl et al. 2016).

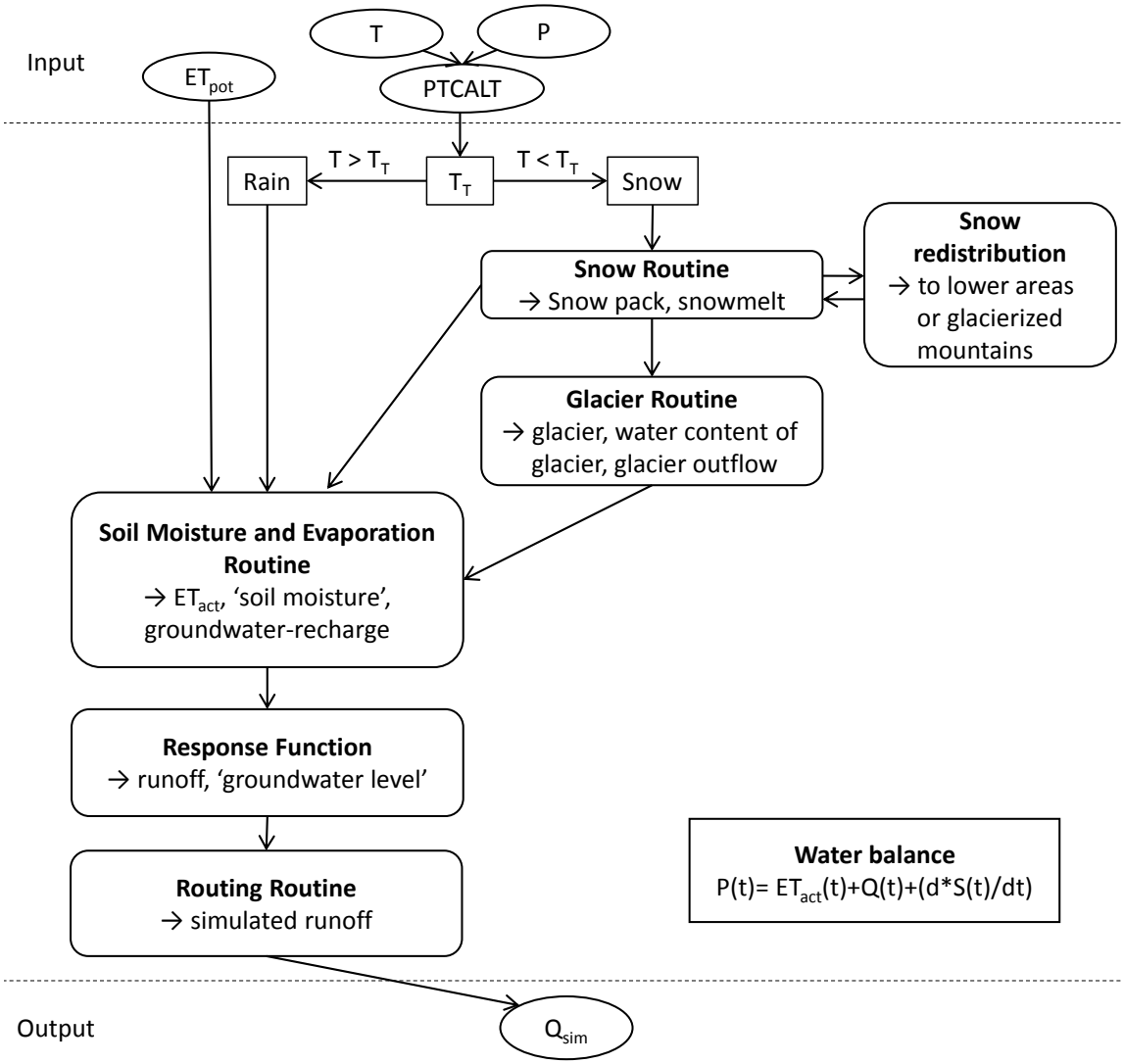

Figure 2.3: Schematic structure of the HBV-light model. (T = air temperature [°C], P = precipitation [mm], ET_{pot} = potential evapotranspiration [mm], ET_{act} = actual evapotranspiration [mm], PTCALT = precipitation [%/100m] and temperature gradients [°C/100m] , T_T = threshold temperature [°C], Q = discharge [mm], S = storage [mm], t = time.)

HBV-light was applied using the standard model structure in the routing routine, an additional snow redistribution and the glacier option, as the catchments are significantly influenced by glaciers. Both, the glacierized and the non-glacierized areas, were subdivided according to their aspect in three categories: North, South and East/West as insolation is crucial for temperatures and melting processes. Vertically, the catchments were classified in 100 m elevation zones.

The warm-up period started in 1973, where initial glacier volume values simulated

by Huss (Huss et al. 2010) based on aerial surveys by Müller et al. (1976). The percentage of the simulated glacier volume by Huss in 1973 of the for the ASG-project reconstructed glacier volume in 1900 was detected. As initial value for the glacier volume simulation in 1973 the corresponding percentage from the look-up table, that was generated by HBV-light in the ASG-project (Stahl et al. 2016), where simulations started in 1900, were used. The start value was taken from the glacier look-up table as glaciers were partly having positive mass balances. To appropriately use the Δh-approach by Huss et al. (2010) the look-up table needed to have the capacity to allow positive mass balances in the 1970s. Furthermore, values are better comparable to the ASG-project (Stahl et al. 2016).

Calibration within the rest of the observation data period from 1976-2006 was then done by optimizing a weighted objective function, giving special attention to streamflow dynamics (50%), snow simulation (25%) and glacier volume change (25%). The Lindstrom measure was used for the streamflow's general dynamic and volume errors, while the Nash-Sutcliffe efficiency was used for logarithmic streamflow during winter low flows and the stream flow peaks during the summer. For calibration of the snow simulations the snow cover area was used as well as the mean snow water equivalent of the elevation range between 2000-2500 m, which is the crucial elevation range for the snow line. Glacier volume was considered in the calibration process using aggregated catchment glacier volumes as simulated by Huss et al. (2010) (1973) and Paul et al. (2011) (2003). Based on that, 10 calibration runs consisting of about 3000 Monte-Carlo simulations and 1000 Genetic Algorithm and Powell optimization (GAP) runs with differing parameter combinations were conducted. The multi-criteria calibration performed well in the ASG project and similarly well for the shorter time period in this study. Acceptable accordance between the simulated and observed data of streamflow, snow and glaciers were achieved.

The final simulations were then run using the most suitable parameter set identified in the calibration runs. The simulation period is 1. Oct. 1976 to 31. Dec. 2099. Two scenarios (RCP 4.5 and RCP 8.5) of the ten different RCMs, each non-corrected (raw) and bias corrected (BC) (using the two different bias correction methods univariate Quantile Delta Mapping (QDM) (Cannon et al. 2015) and multivariate bias correction (MBCn) (Cannon 2017)), were used. Evaluating the four catchments Hinterrhein, Landquart, Schwarze and Weisse Lütschine, this led to 240 model runs in total:

$$4catchments * 10RCMs * 2RCPs * (raw + 2BC) = 240runs \tag{7}$$

3 Results

3.1 Results of the bias correction

Correcting the RCMs' temperature and precipitation data towards the reference data is a necessary data preparation step. RCMs are based on physical processes and therefore never produce historical values, yet statistical values of a time series should match the reference. Depending on the RCM and the catchment, partially large differences were detected between the RCM model output and the corrected HYRAS reference dataset. In the case of this study, air temperatures were underestimated by up to 6 K and precipitation was overestimated by up to 100%. Exemplarily, the reference data and the results of one uncorrected RCM (CCLM4-8-17 (GCM: CNRM-CM5-LR) run by the CLM community (table 2.2)) are shown for the Hinterrhein catchment in the first two columns of Figure 3.1. It is clearly visible, that the marginal distribution and the range of both daily air temperature (T_a [°C]) (a, b) and daily precipitation amount (P [mm]) (m, n) do not match the reference data and need to be corrected. After applying the two chosen bias correction methods (multivariate bias correction (MBCn) and univariate quantile delta mapping (QDM)) the RCMs' marginal distributions match the reference data much better and perform equally well (Figure 3.1 c, d, o, p).

However, the two bias correction methods show differences concerning the representation of the interdependence of air temperature and precipitation. In Figure 3.1 slight differences are visible in the bivariate scatterplots including the local regression line (second row, e-h) and in the density distribution (third row, i-l) of the variables' co-occurrence. The local regression lines as well as the highest densities vary around air temperatures of 0°C. As argued before, the correct representation of precipitation around 0°C is of special importance for the simulation of the snow or glacier accumulation and is therefore especially focused on.

Analyses of the annual precipitation in dependence of air temperature have been conducted. The 11-year moving average of the number of days per year (N[d]) with precipitation at air temperatures (T[a]) above (Fig. 3.2 a) and below or equal to 0°C (Fig. 3.2 b) is displayed in Figure 3.2. Accordingly, the 11-year moving average of the annual precipitation amounts at air temperatures above (Fig. 3.2 c) and below or equal to 0°C (Fig. 3.2 d) were extracted and summarized. For the Hinterrhein catchment it is evident that the number of days with precipitation when air temperatures are below or equal to 0°C is higher for the MBCn corrected data (100-120 days per year) compared to the QDM corrected RCM data that vary roughly from 80 to 110 days per year. The precipitation amounts vary accordingly. At air temperatures below or equal to 0°C they are higher for the MBCn corrected data in comparison to the QDM corrected data. The 11-year moving average of annual precipitation amounts varies between 900 - 1200 mm/yr for MBCn corrected RCM data and between 500 - 1000 mm/y for QDM corrected RCM data. Precipitation amounts above 0°C vary for the MBCn corrected data between approximately 1000 - 1200 mm/yr and lie below the annual precipitation amounts of 1200-1600 mm/yr generated by the QDM corrected data. Hence, the QDM corrected data have a wider variation

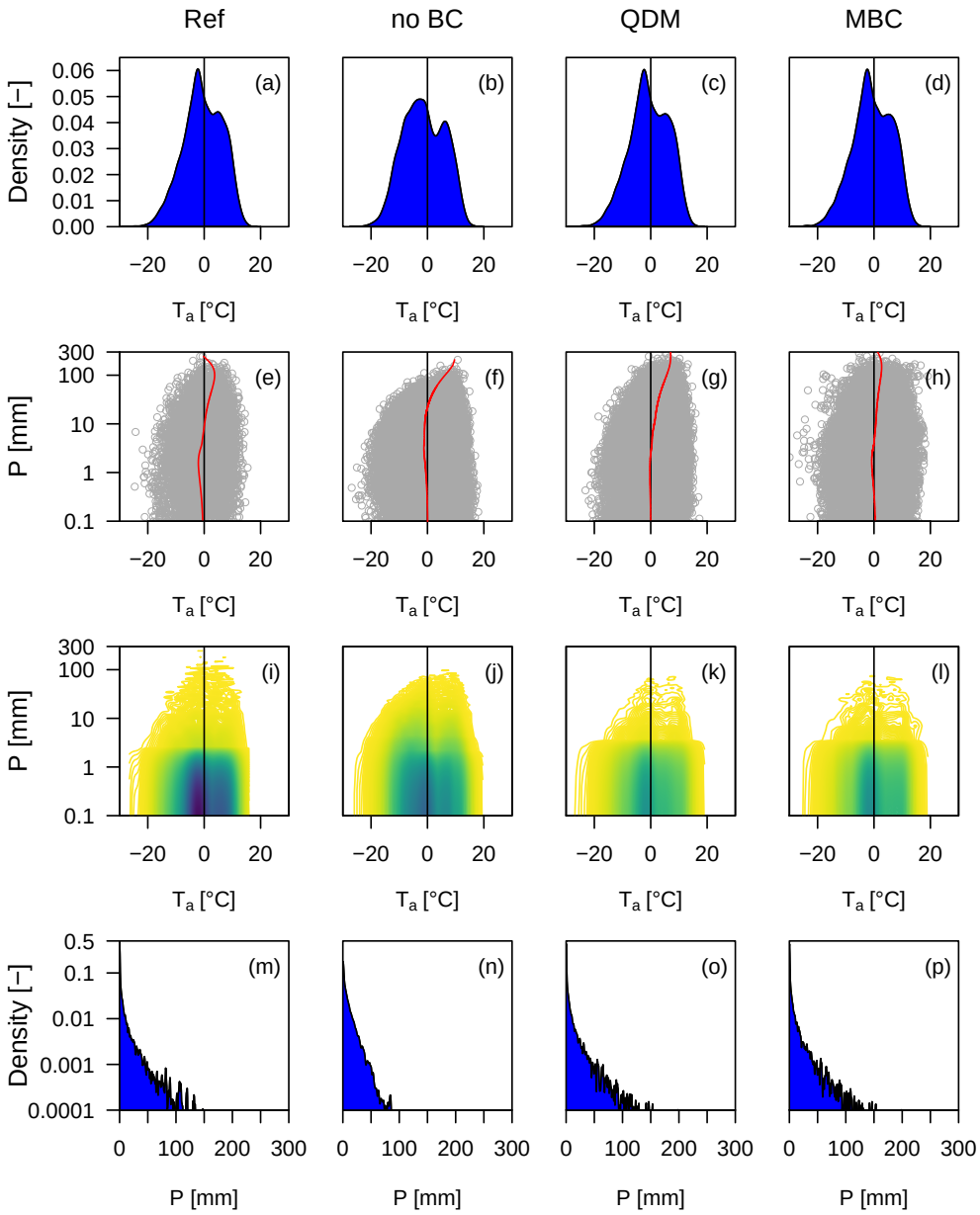

Figure 3.1: Exemplary representation of the climate variable's air temperature (T_a) and precipitation (P) of one RCM in the Hinterrhein catchment during the calibration period (1977-2006). The cumulative distribution of air temperature is shown in the top row (a-d), while the cumulative distribution of precipitation is shown in the bottom row (m-p). The bivariate plots in the middle rows show the co-occurrence of air temperature and precipitation, showing the local regression line (e-h) and the density allocation (i-l). The left column (a, e, i, m) represents the reference data, the second column (b, f, j, n) the uncorrected RCM data, the third column (c, g, k, o) the QDM corrected data and the right column (d, h, l, p) represents the MBCn corrected data.

than the MBCn corrected data. While the precipitation amounts and the number of days per year vary for the other three catchments of Landquart, Schwarze and Weisse Lütschine, the variance of the RCMs and the general distribution of MBCn and QDM corrected data stays similar. The corresponding figures for the other catchments are shown in the appendix B2.

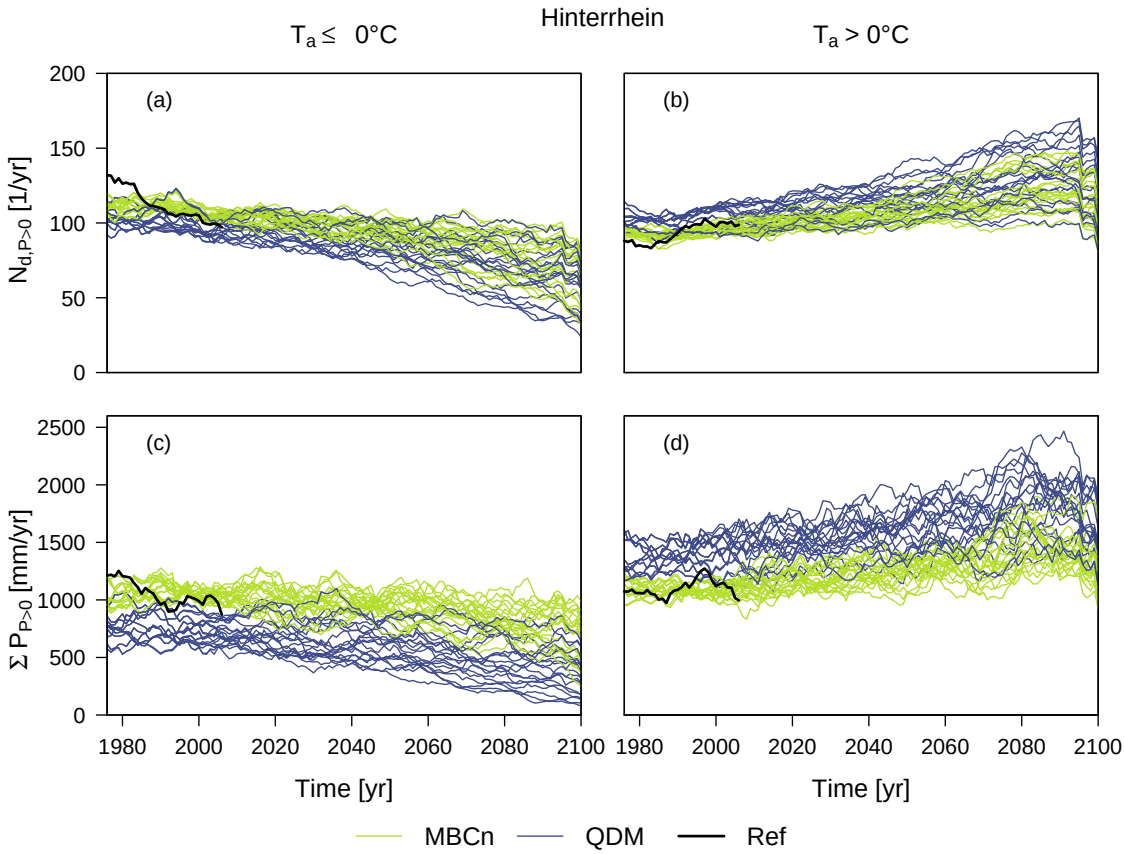

Figure 3.2: Representation of the 11-year moving average of the annual number of days with precipitation (P [N_d/yr], top row (a, b)) as well as the annual precipitation amount (P [mm/yr], bottom row) at air temperatures (T_a) below (left column (a, c)) or above 0°C (right column (b, d)) over time (1977-2100) for the Hinterrhein catchment. The twenty different lines represent the ten different RCMs, each corrected with QDM and MBCn. The bold black line represents the calibration simulation (sim_{cal}) based on reference values.

Furthermore, temperatures on dry days were evaluated (Fig. 3.3, appendix B3). Results are not as distinct as they are for the days with precipitation. However, tendencies are the same. While there are around 80-90 dry days per year with air temperatures below or equal to 0°C for the MBCn corrected RCM data, 90-100 dry days are simulated with QDM corrected RCM data. Correspondingly, MBCn corrected data show 75-85 dry days per year at air temperatures above 0°C, while only 60-80 dry days per year at air temperatures above 0°C are simulated using QDM corrected data. Concerning the mean temperatures on dry days below 0°C, they are slightly warmer (-6 - -5°C) for MBCn corrected data compared to QDM corrected

data (-8 - -6°C). However, no difference in the mean daily temperature is visible for temperatures above 0°C on dry days. Both correction methods vary around mean temperatures of 5°C.

The corrected HYRAS reference data, towards which the RCMs are corrected, lie rather within the range of the MBCn corrected data. As no differences between the correction methods are visible concerning the marginal distributions of the individual variables (Figure 3.1), differences become more distinct regarding the co-occurrence of precipitation and air temperature (Figures 3.2 and 3.3). This is an indication for the assumption that MBCn gives the more realistic results.

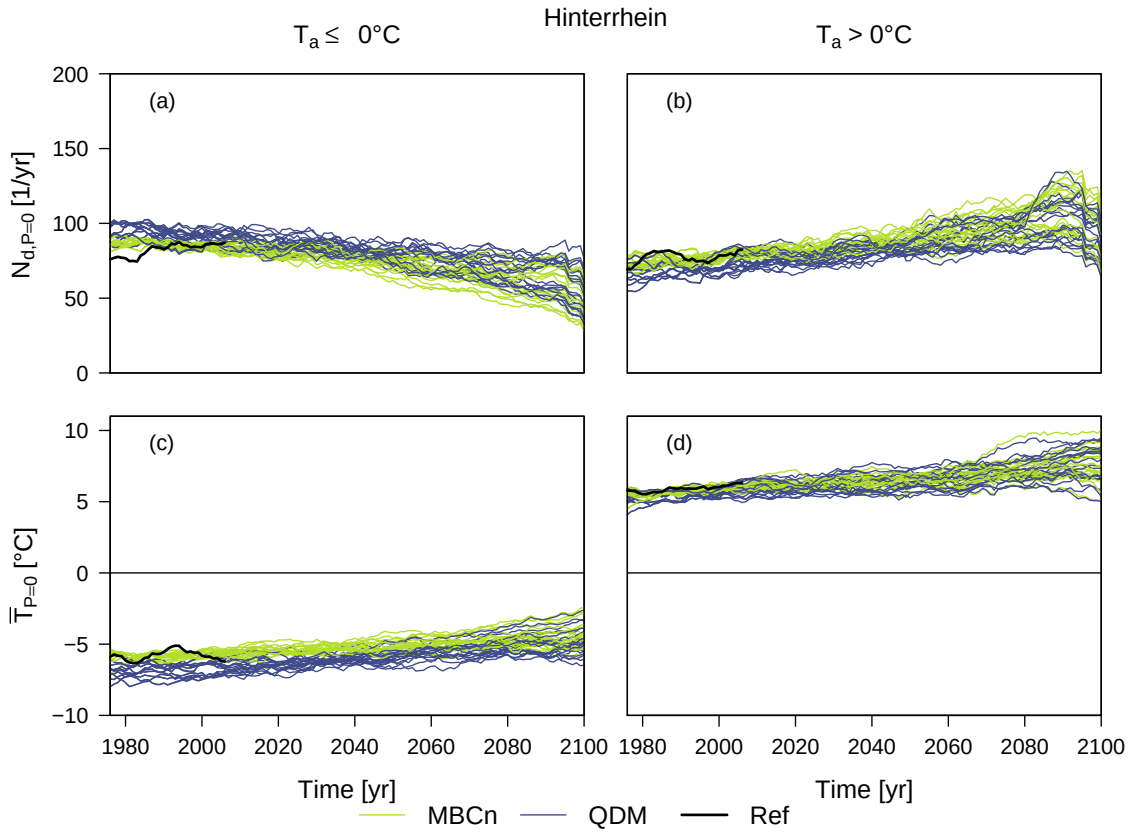

Figure 3.3: Representation of the 11-year moving average of the annual number of days without precipitation ($N_{d,P=0mm,T\leq/>0°C}$ [1/yr], top row (a, b)) as well as the annual mean temperatures on days without precipitation ($\overline{T}_{P=0mm,T\leq/>0°C}$ [mm/yr], bottom row) at air temperatures (T_a) below (left column (a, c)) or above 0°C (right column (b, d)) over time (1977-2100) for the Hinterrhein catchment. The twenty different lines represent the ten different RCMs, each corrected with QDM and MBCn. The bold black line represents the calibration simulation (sim_{cal}) based on reference values.

3.2 HBV-light simulation results

3.2.1 Impacts of the bias correction method

The differences in the interdependence of precipitation and temperature introduced by the use of different multi- and univariate bias correction methods (MBCn, QDM) applied to the RCM data, can be traced for instance in the snow water equivalent (SWE) modelled in HBV-light. The nature of precipitation being solid or liquid is of special importance for the snow accumulation and therefore leads to differences in the annual SWE regime. The more precipitation is simulated at air temperatures below 0°C, the more falls as snow and accumulates. Accordingly, as MBCn corrected RCM data imply more precipitation falling as snow, a higher SWE is simulated, compared to simulations based on QDM corrected data. There is a strikingly clear distinction of simulated SWE based on different bias correction methods. The calibration simulation based on the reference climate data separates the results of simulations with both correction methods and does not allow a clear conclusion to which bias correction method performs better. The distinction of the bias correction methods is a little less clear for other catchments of the time period in the future, yet the tendencies in method performance are obvious. The clear distinction of the 11-day moving average of the annual SWE simulations is displayed in Figure 3.4 (appendix C1), where the annual SWE regime is illustrated for the historic (1977-2006) time period on the left (a, c) and the future time period (2070-2099) on the right (b, d), further separated into the RCP 4.5 scenario at the top (a, b) and the RCP 8.5 scenario at the bottom (c, d).

The simulations of glacier retreat show similar tendencies as the SWE using differently corrected RCM data. Again, MBCn corrected data show a slower glacier retreat in comparison to simulations based on QDM corrected RCM data. However, the distinction of the differently corrected RCM data is not as clear for glacier volume simulations as it is for the SWE regimes. Especially from the middle of the 21^{st} century the correction methods mix as RCMs in general diverge over the simulation period until 2100. However, for each individual RCM glacier melt is faster using the QDM corrected data compared to MBCn corrected data. Figure 3.5 shows the simulated glacier volume for the two RCP scenarios (RCP 4.5 (left column, a, c, e, g) and RCP 8.5 (right column, b, d, f, h)) over the simulation period in the four modelled catchments Hinterrhein (top row, a-b), Landquart (second row, c-d), Schwarze Lütschine (third row, e-f) and Weisse Lütschine (bottom row, g-h). As reference the HBV-light calibration simulation based on observed data was added, as well as points for glacier volume acquisitions by Paul et al. (2011) (2003) and Huss et al. (2010) (2010, upper point) and Fischer et al. (2014) (2010, lower point).

Changes deriving from different bias correction methods also transfer into streamflow simulations. Simulations based on QDM corrected data always show more streamflow than MBCn corrected data. This makes a difference of up to 150 mm in the mean annual runoff. Yet, differences are more pronounced regarding the individual runoff components. Modelling based on QDM corrected RCM data show a more than 10% higher runoff component for direct runoff from rainfall in comparison to

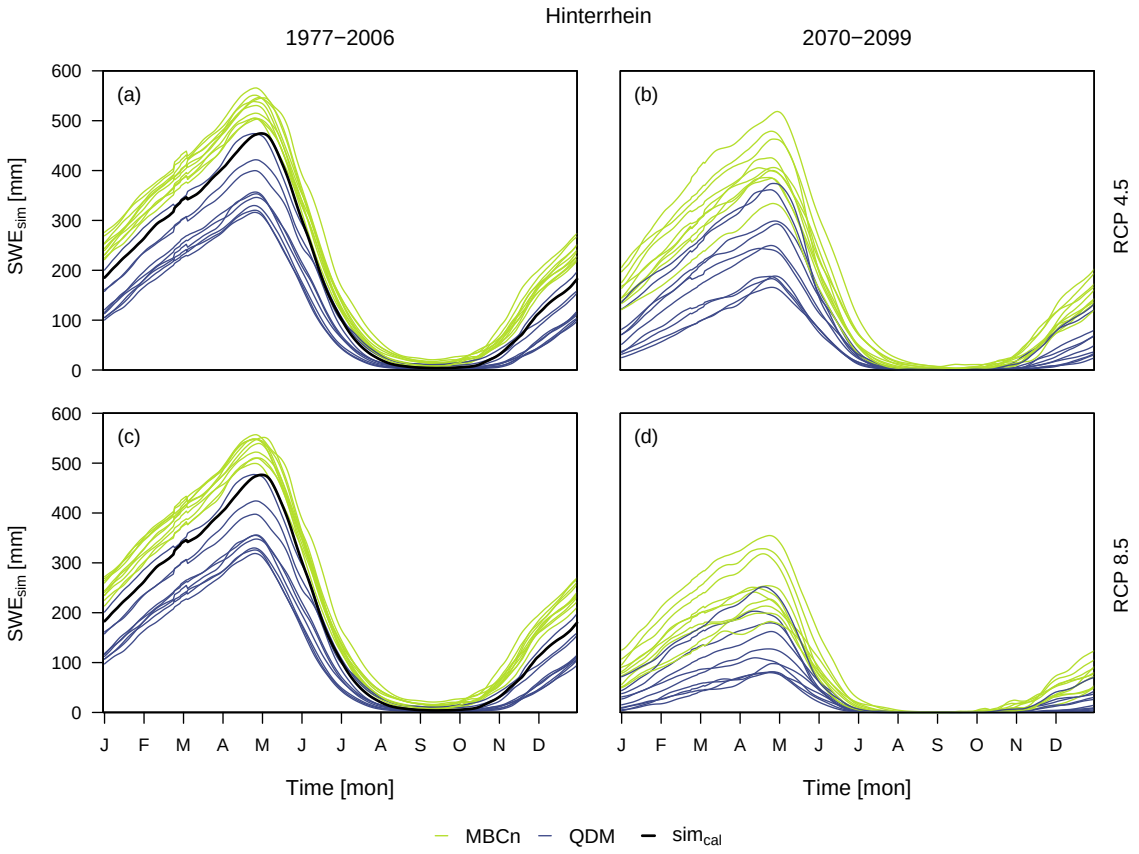

Figure 3.4: Annual snow accumulation regime, calculated using the 11-day moving average of the daily simulated SWE for the Hinterrhein catchment. The average was built for two 30-year periods during the calibration period from 1977-2006 (column on the left (a, c)) and the projected period from 2070-2099 (column on the right (b, d). The two different scenarios for which the simulation was conducted are the RCP 4.5 scenario in the top row and the RCP 8.5 scenario in the bottom row. The 20 different lines represent the 10 RCMs, each corrected with QDM and MBCn.

MBCn corrected data simulations. The snowmelt runoff component varies proportionally, being significantly smaller for models using QDM corrected RCM data. No differences deriving from bias correction methods is detected for the glacier runoff component. These differences are best shown in Figure 3.6 (appendix C2).

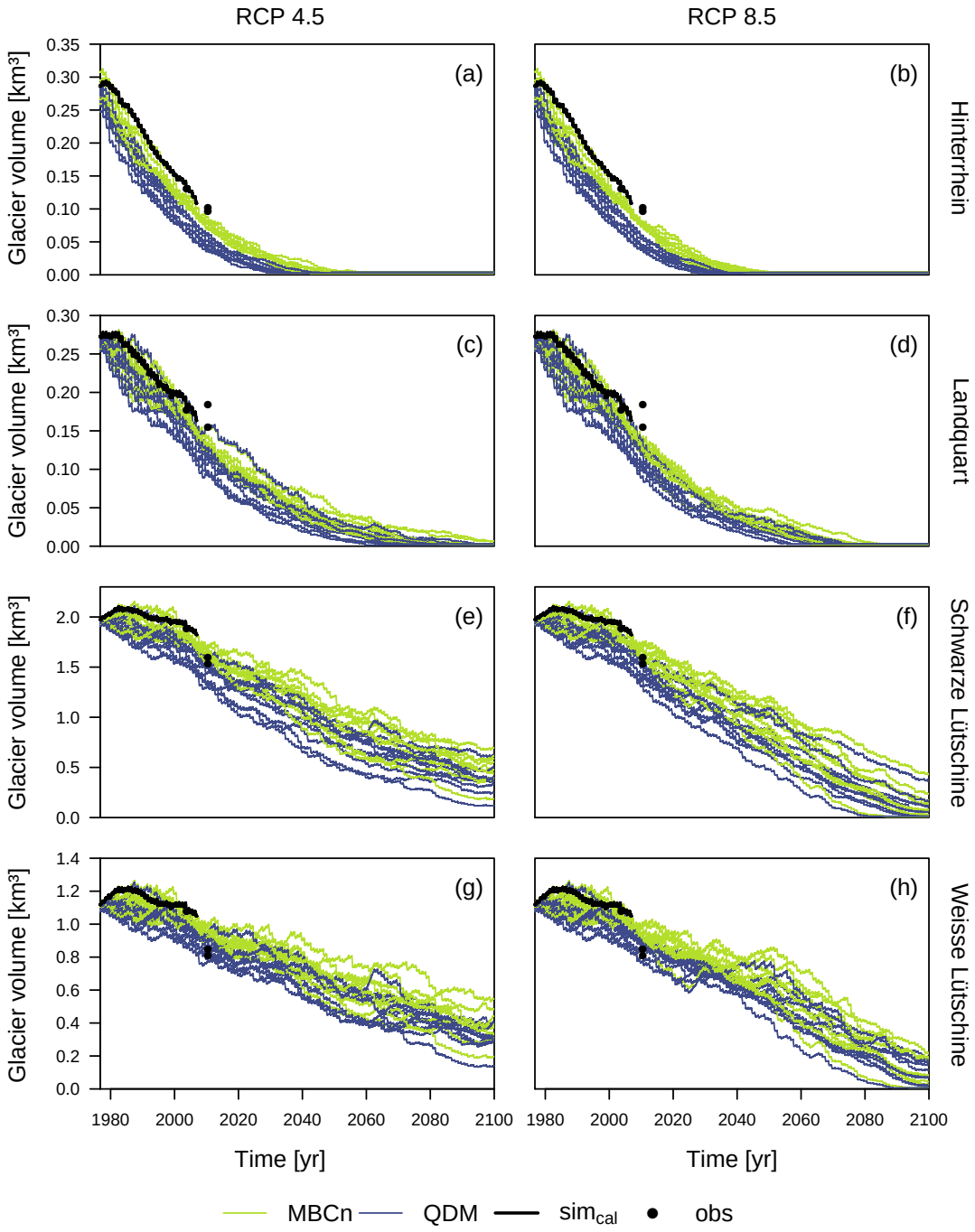

Figure 3.5: Simulated glacier volume over time from 1977-2100 in the four evaluated catchments (Hinterrhein (top row, a, b), Landquart (second row, c, d), Schwarze Lütschine (third row, e, f) and Weisse Lütschine (bottom row, g, h). The 20 lines represent the 10 RCMs, coloured based on the applied bias correction method (QDM, MBCn). In comparison the glacier volume simulated using observed values is displayed in black and observed values by Paul et al. (2011) (2003), Huss et al. (2010) (2010, upper point) and Fischer et al. (2014) (2010, lower point) are added as black points.

3.2.2 Impacts of changing climate

Based on the RCM data, trends in the annual snow accumulation can be observed (Fig. 3.4, appendix C1). The most intuitive change is a smaller snow accumulation in the course of a year for the future time period (2070-2099) in comparison to the historic time period (1977-2006) and a more complete melt during the summer. This extends the snow free period during the summer, especially for the RCP 8.5 scenario. The onset of the snow accumulation occurs later in the course of a year while the melting finishes earlier. The variation in the different RCMs diverges for the future simulations. Respectively to the design of the RCP scenarios, RCP 8.5 simulates 40-70% less SWE in the future time period in comparison to RCP 4.5 that simulates 10-50% less SWE.

In the course of the simulation period from 1976-2100 the glacier volume retreats in all catchments. In the Hinterrhein catchment, glaciers diminish continuously from the beginning of the simulation period for both, the RCP 4.5 and the RCP 8.5 scenario and are simulated to have disappeared between 2030 and 2055 depending on the bias correction method applied to the RCM data and the RCMs. In the other catchments, there is stagnation or an increase in glacier volume in the 1970s or in the beginning of the 1980s. In the Landquart catchment glaciers retreat after a stagnant period that lasts for only 10 years in the beginning of the simulation period. Some RCMs project a full wastage of glaciers by the end of the 21^{st} century from 2070, others do not model the complete wastage within the simulation period under the RCP 4.5 scenario. However, assuming the RCP 8.5 scenario, all glaciers in the Landquart catchments will have melted before 2080. In the Lütschine catchments several RCMs simulate an increase in glacier volume in the 1970s and 1980s, which is in line with the calibration simulation. Afterwards, glaciers retreat even for the catchments at high altitudes. Other than in the Hinterrhein and partly the Landquart catchment, glaciers are not simulated to have diminished by 2100 assuming the RCP 4.5 scenario. However, they shrink to roughly a third of their size at the beginning of the simulation period. Assuming the RCP 8.5 scenario, simulations based on certain RCMs simulate even the Schwarze and Weisse Lütschine catchments to be glacier free. The glacier retreat is shown in Figure 3.5.

Trends during the simulation period were also simulated for the total runoff that seems to stay relatively constant over the simulated time period from 1976 to 2100 in all four modelled catchments. Hinterrhein, Landquart and Schwarze Lütschine have a total discharge of roughly 1800-2000 mm/yr, while about 500 mm/yr less drain in the Weisse Lütschine. However, the further into the future, the more the simulations based on different RCMs diverge. Some simulations denote a slight decrease in discharge, while others indicate increasing values. These differences appear to be part of the RCMs increasing modelled variations. The 11-year moving average of the annual runoff sums split into the three runoff components (rainfall Q_R, snowmelt (Q_S) and ice melt (Q_I)) over the entire time period from 1976-2100 are shown in Figure 3.7 for the Hinterrhein and averages for three different time periods in Figure 3.6. The runoff sums including the runoff components over time for the other three catchments are shown in the appendix C2 and C3.

While the total annual runoff stays largely unchanged, the composition of the

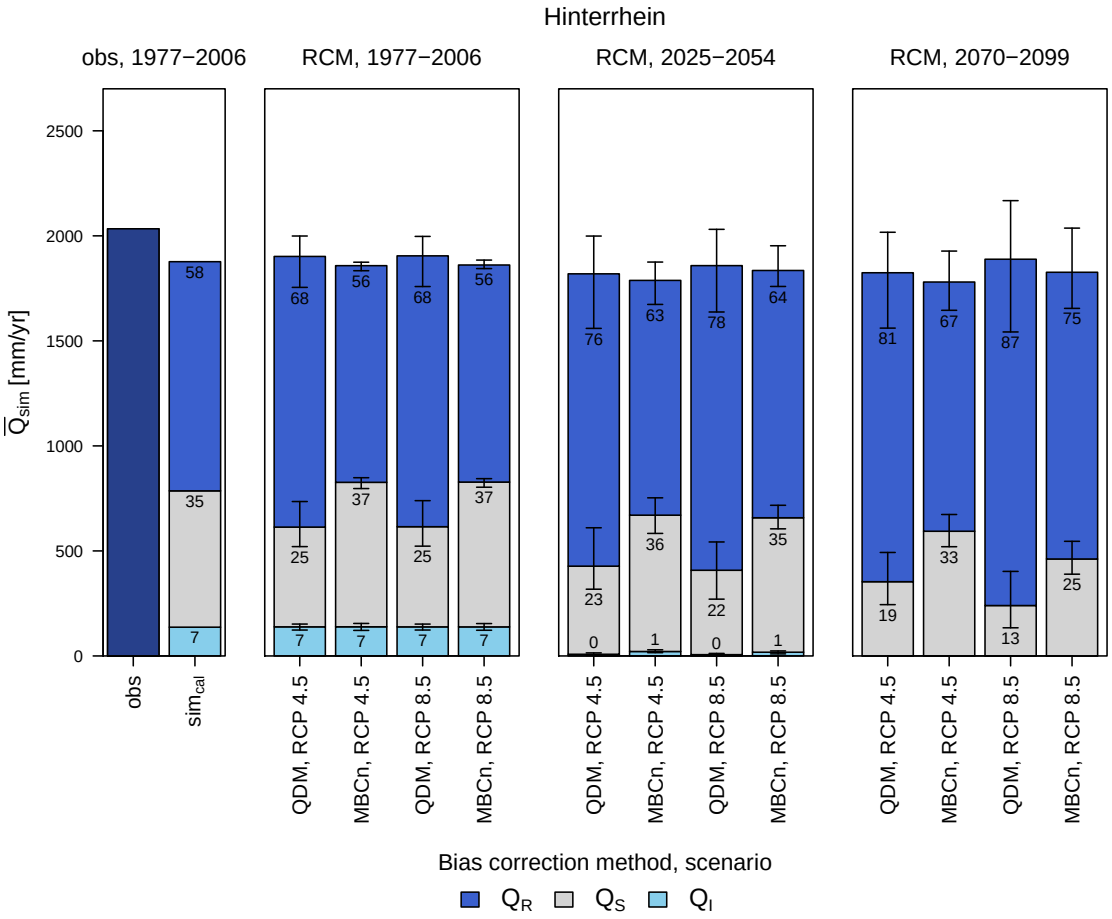

Figure 3.6: Mean runoff sums simulated using different climate variable input bias correction methods (QDM, MBC) and different RCP-scenarios (RCP 4.5, RCP 8.5) in the Hinterrhein catchment. The total runoff is split into its three components: ice melt (Q_I, bottom), snowmelt (Q_S, middle) and rainfall (Q_R, top) and their percentages of the total runoff are indicated. The error bars at the top of each section indicate the minimum and maximum mean results achieved from the 10 RCMs. The means of three different 30-year time periods are shown: the historic time period from 1977-2006 on the left, one time period in the near future (2025-2054, middle) and the one at the end of the 21^{st} century (2070-2099) on the right. In comparison the observed runoff (obs) and the runoff simulated using observed input data (sim_{cal}) are displayed on the left.

runoff changes. The biggest and in absolute quantities most uncertain runoff component is the one deriving from rainfall. One striking variance in the rain induced runoff component is the bias correction method applied to the RCM data. Generally, QDM corrected RCM data simulate a 12-14% higher rainfall component than MBCn corrected data for the Hinterrhein. In the Hinterrhein catchment rainfall induced runoff made up roughly 60% of the runoff during the historical time period from 1977-2006. Until the end of the 21^{st} century it is simulated to increase to 70-80% or even to around 90% for some simulations based on QDM-corrected RCM

data under the RCP 8.5-scenario. Simulations using MBCn corrected data simulate on average 67% rainfall induced runoff for the RCP 4.5 scenario and a little more, around 75% for the RCP 8.5 scenario. The rainfall parts are correspondingly higher for the simulations based on the QDM corrected data, being around 81% for the RCP 4.5 scenario and around 87% for the RCP 8.5-scenario. Generally, variations of the rainfall induced runoff part deriving from different RCMs increase towards the end of the 21^{st} century. The other three catchments show similar tendencies, yet, the rainfall induced runoff part is smaller in general and simulated to increase less.

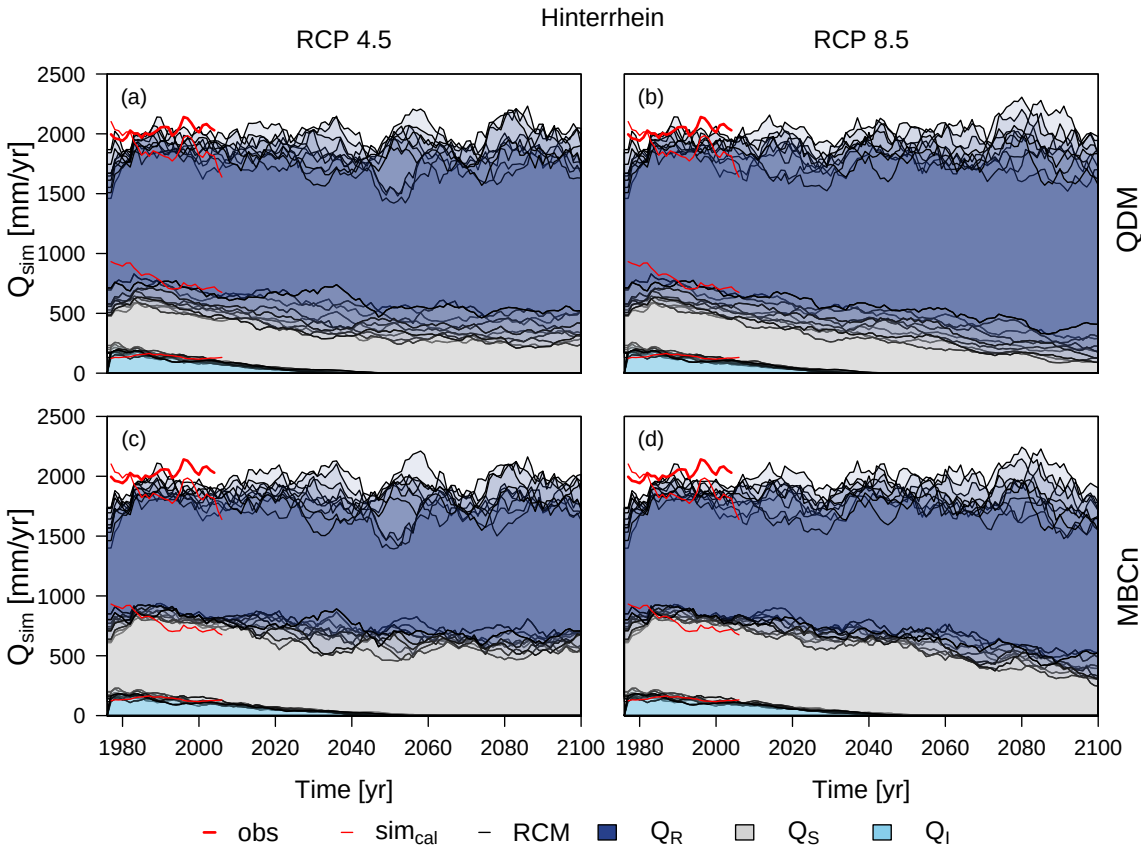

Figure 3.7: 11-year moving average of annual runoff sums for the Hinterrhein catchment from 1977-2100. The simulated total runoff is split into its three components of origin: rainfall (Q_R), snowmelt water (Q_S) and glaciermelt water (Q_I) and is compared to observed runoff data (obs) and the simulation results based on observed data (sim_{cal}) during the historic period (1977-2006). The left column (a, c) shows results simulated based on the RCP 4.5 scenario, whereas in the right column (b, d) the RCP 8.5 scenario is displayed. In the top row (a, b) simulation results modelled with QDM corrected data are shown, compared to simulation results using MBCn corrected data in the bottom row (c, d).

Alike the rainfall component, the snowmelt component of the total runoff shows clear differences in the HBV-light results depending on the RCM and the bias correction method applied. During the historic period from 1977-2006, the HBV-light calibration simulation, using the reference climate data, simulated 649 mm/yr (35%)

snowmelt part of the annual Hinterrhein runoff (Q_{tot}). For QDM corrected RCM model data, 475 mm/yr (25% of Q_{tot}) snowmelt runoff were simulated, while MBCn corrected data are closer to the calibration modelling and simulate 688 mm/yr (37%) snowmelt runoff. Over time until the time period from 2070-2099, the snowmelt component decreases by 25-50% to 353 mm/yr (19%), assuming the RCP 4.5 scenario or to 240 mm/yr (13%) assuming the RCP 8.5 scenario for the QDM corrected RCM data. Using MBCn corrected RCM data a much smaller decrease in snowmelt runoff is simulated. Assuming the RCP 4.5 scenario, the snowmelt component decreases by 10% to 594 mm/yr (33%), by 32% to 462 mm/yr (25%) assuming the RCP 8.5 scenario. The mean snow runoff part in the time period from 2070-2099 is higher for MBCn corrected data than for QDM corrected data during the historic period from 1977-2006. However, all combinations of RCM data, bias correction method and scenario show a slight decrease in snowmelt runoff. Similar results with decreasing absolute and relative snowmelt runoff parts are obtained for all catchments. The other three catchments have generally higher snowmelt runoff parts than the Hinterrhein and the relative decrease is less.

In the Hinterrhein catchment the glacier retreats quickly and so does the runoff part generated by ice melt. Both RCP scenarios, no matter which correction method was applied to the RCM data, show consistent results of a decreasing glacier melt runoff and the final stop between 2030 and latest 2055. During the historic period from 1977-2006, ice melt runoff corresponds on average to 7% of the annual runoff, which equates to an absolute value of just under 140 mm/yr. For Landquart the runoff part of glacier meltwater is generally rather small, being just under 60 mm/yr, which is equivalent to 3% of the total annual runoff. The ice melt runoff component for Landquart will be gone towards the end of the 21st century (2060-2080), but is too small to influence the characteristics of the general annual runoff even before that. For the Schwarze Lütschine a slight increase of about 50 mm/yr in the glacier melt water induced runoff part can be observed during the calibration period from 1977-2006 averaging 12% of the total annual runoff. Afterwards, the glacier runoff part stays rather stable and constant for 3-4 decades, before it starts decreasing towards the end of the 21st century. Until the period of 2070-2099 a decrease of roughly 50-60% in comparison to the historic time period from 1977-2006 to 75-110 mm/y (4-6%) is simulated to have taken place. The glacier runoff part in the Weisse Lütschine shows a similar behaviour as the one in the Schwarze Lütschine. A slight increase in ice melt water runoff until the end of the calibration period (1977-2006) can be observed, before the glacier runoff part stays at a stable level. In the second half of the 21^{st} century, glacier runoff starts to continuously decrease. In total, there is a decrease in 40-50% to 70-95 mm/yr comparing the historic calibration period (1977-2006) and the projected period (2070-2099).

However, not only does the annual runoff change during the simulation period from 1976 until 2100, intra-annual variations are altered as well. In the past (1977-2006) all catchments showed a glacio-nival regime peaking around June with little runoff during winter. The glaciers' influence shows during late summer, where it extends the snowmelt peak into autumn. With vanishing ice melt runoff, the runoff peak during June will be more pointed in the future towards the end of the simulation period (2070-2099) and water levels in late summer are simulated to be lower. Also

in winter runoff gets higher on average in the future time period from 2070-2099. This is shown in Figure 3.8 (appendix C4), where the 11-day moving average of the annual regime as well as the simulated runoff components averaged over 30-year periods are displayed.

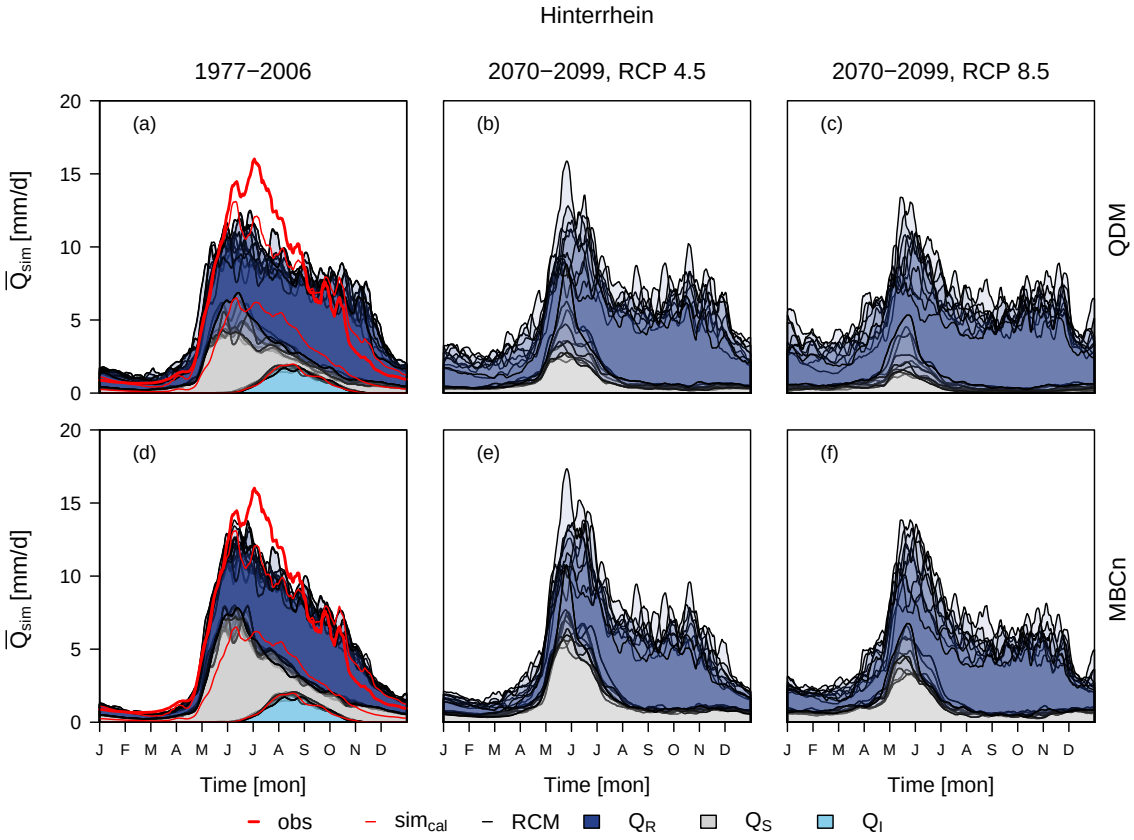

Figure 3.8: Runoff regimes using 11-day moving averages of daily runoff for the Hinterrhein catchment during 30-year periods in the past (1977-2006) and future (2070-2099) for the two scenarios RCP 4.5 and RCP 8.5. The simulated runoff is split into its three components of origin: rainfall (Q_R), snowmelt water (Q_S) and glacier melt water (Q_I) and is compared to observed runoff data (obs) and the simulation results based on observed data (sim_{cal}) during the historic period. The left column (a, d) shows the results during the historic period, while the other two columns represent results for the future time period using the RCP 4.5 scenario (b, e) and the RCP 8.5 scenario (c, f). In the top row (a-c) simulation results modelled with QDM corrected data are shown, compared to simulation results using MBCn corrected data in the bottom row (d-f).

The runoff component due to rainfall is the largest component in the annual runoff with about 60-80%. In absolute values it contributes most during the summer and autumn, while during winter only little runoff is generated in general. However, the average rainfall induced runoff component in the future time period from 2070-2099 will be higher in comparison to the past time period from 1977-2006. For the Hinterrhein catchment a remarkable variation can be observed in the rain induced

runoff parts for both, the historical 30-year time period from 1977-2006 and in both simulated RCP-scenarios in the future time period from 2070-2099, even though the mean runoff is smoothed using an 11-day moving average. The other three catchments show less variation in the smoothed runoff. The tendencies of a larger absolute rainfall component in winter the consequently a higher total winter runoff is clearly visible in all catchments.

The snowmelt component peaks in late spring, where it takes up about 50% of the runoff. During the rest of the year the runoff due to snowmelt is rather small taking up only a little percentage. This snowmelt determines the catchments' runoff characteristics and will not lose its significance in the future. As shown before in Figure 3.7 the annual snowmelt amount is simulated to decrease in the future. However, during the snowmelt peak in late spring, the absolute snowmelt part of the total runoff increases in some cases leading to a higher and more pointed snowmelt peak. However, large differences in the snowmelt component can also be observed depending on the bias correction method applied to the RCM data. As more snow accumulation is simulated for MBCn corrected RCM data, more runoff due to snowmelt is simulated in comparison to less snowmelt and an accordingly smaller snowmelt runoff component for QDM corrected RCM data. No significant temporal shift of the snowmelt peak occurring earlier in spring can be observed.

The third runoff component, the runoff induced by glacier ice melt, constitutes a rather small part of the total runoff, making up only 7% during the reference period in the Hinterrhein catchment. However, during the calibration period (1977-2006) the glacier runoff was of major importance during late summer, where it peaks at around 20% of the runoff. The glacier runoff component is the most noticeable difference comparing the historic runoff regime to the future runoff regime. While the glacier melt water made up around 20% of the total runoff during the late summer in the past, it will be completely gone with the diminishing glacier, leading to considerably less total runoff during late summer. While in Hinterrhein and Landquart the glaciers will melt away completely during the simulated time period, the Schwarze and Weisse Lütschine will continue to have runoff originating from glacier meltwater, however reduced by $\sim$ 10% in the late summer from former almost 30% to less than 20% by the end of the simulation period (2070-2100).

4 Discussion

4.1 Differences resulting from bias correction

RCMs often have substantial biases when simulating climate. Nevertheless, they are a useful and trustworthy tool to assess changes in future climate. However, raw RCM output should be used only with caution or best, being corrected, when applied in climate change impact studies, e.g. in the hydrological field. The necessity of bias correction is demonstrated in the following example for RCM 8 (IPSL-CM5A-MR, RCA4), scenario RCP 8.5, in the Weisse Lütschine catchment. As illustrated in Figure 4.1 the scenario of generally warming climate is plausibly represented within the temperature time series, however, there is a constant negative bias and air temperatures are underestimated by around 6 K in the raw RCM output data. Applying either correction method (MBCn or QDM), the output's temperature can be lifted to the observed data. Precipitation, on the contrary, was overestimated by 1500-2000 mm and corrected to values close to observations. Simulating these raw data in HBV-light leads to a runoff, that shows an extreme and unrealistic increase in streamflow from 2040 onward. Tracking down the reason for this it becomes clear, that due to the cold temperatures in the uncorrected dataset, huge amounts of snow accumulated over the years and the glacier volume increased rapidly during the simulations. It is the absolute contrast to what is observed. With even further rising temperatures, as simulated using the RCP 8.5 scenario, the immensely accumulated snow and glacier reservoirs release melt water into the stream. Regarding the general understanding of climate change, it is common sense that the opposite is more likely to happen. Having applied either bias correction technique leads to much more realistic results supporting the current state of knowledge.

Consequently, the following question arises: Where does this substantial bias in the simulated climate variables originate from? The entire RCM ensemble used in this study, had a negative temperature bias (simulations are colder than the reference data) and a positive precipitation bias (simulations show more precipitation than the reference data). In the Alps, weather is often a local phenomenon, that is not completely represented in the RCMs. Physical processes are often simulated in a simplified way and the spatial resolution is often rather coarse (Ehret et al. 2012). Especially the highly complex topography of the Alps is not adequately integrated in the RCMs that are covering entire Europe. The mean altitudes of the simulated and the real mesoscale, alpine catchments in this study differ by several hundred meters.

Correcting biases in the RCM outputs, one has to be careful with the choice of method and be aware of the method's limits. Correcting the RCM output based on a possible origin of a bias was not an option as the biases are a combination of unquantified sources. Further advancement of RCMs is certainly the best way to further improve its output. However, we have to work with the current state of the art. A mean elevation based correction approach was abandoned, because the use of uncertain temperature lapse rates would introduce additional uncertainties to the dataset. As the correction methods applied in this study work exclusively based on statistical methods, they correct all biases, independent of their origin.

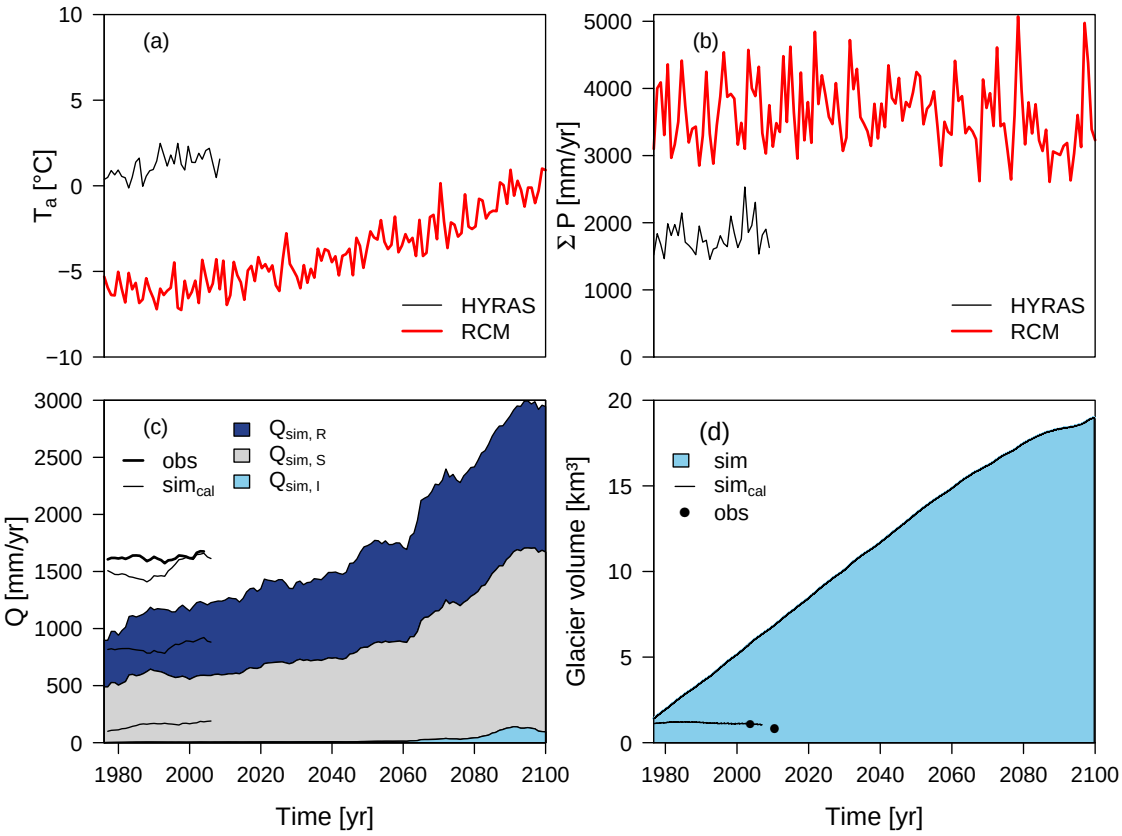

Figure 4.1: Non-corrected RCM data in comparison to reference data in the Weisse Lütschine catchment. Shown are the annual mean temperature (T_a) (a) and the annual precipitation sum (ΣP) (b) of one uncorrected RCM, as well as resulting simulated runoff components (Q) (c) and glacier volume (d).

Yet, there are significant differences even though both applied correction methods, the univariate Quantile Delta Mapping (QDM) and the multivariate bias correction (MBCn), work based on statistics only. The core of both correction methods is QDM, which aims to correct the marginal distribution of the climate variables. Therefore it is in the nature of the correction methods that the target distributions are reproduced equally well achieving similarly good results for individual climate variables (chapter 3.1, Fig. 3.1). However, it comes to clear distinctions of the bias correction methods, when comparing their performance in correcting the interdependence of the climate variables that plays a crucial role in alpine catchments. QDM is a univariate correction method and does not consider the variables' interdependence. MBCn differs from QDM through the rotation of the source, projection and target datasets. Owing to the generated linear combinations, the climate variables' interdependence is preserved and matches observation data better.

These differences that occur through the climate variables' interdependencies transfer into hydrological modelling. As previously shown, differences in the texture of precipitation based on temperatures above or below 0°C (Fig. 3.2) lead to differences in snow accumulation (Fig. 3.4). Distinctively more snow accumulation is

simulated using multivariate corrected climate model data, that also simulate more precipitation falling as snow. The minimum SWE simulated based on MBCn corrected RCMs is higher than the maximum SWE modelled using QDM corrected climate model data. Consequently, a clear difference in SWE is introduced by the bias correction method. In comparison to the observed data it is striking that it lays in between the simulations using the two correction methods. While QDM corrected data based simulations model too little snow, it is not easy to explain the higher snow accumulation for simulations based on MBCn corrected data. Maybe there is a little more sublimation or melting that is not represented in the simulations using MBCn corrected data. Concerning glacier simulations, similar tendencies are visible. Considering each RCM individually, QDM corrected data always simulate less glacier volume than MBCn corrected data. However, the bias correction method does not make an as distinct difference as simulated for the SWE and is overshadowed by the RCM variation. This difference in the bias correction method might derive from the slow decrease of the glacier reservoir that is not reacting as sensitive to the interdependence of precipitation and air temperature as the SWE does. Slower glacier retreat for MBCn corrected data might be the result of later occurring glacier melt as more snow is accumulated that takes longer to clear away. Additionally, HBV-light transforms a certain percentage of the snow layer into glacier ice each year, which slightly countervails glacier ice melt (Stahl et al. 2008). This percentage is higher, when the snow accumulation is more pronounced, and therefore higher for MBCn corrected data in comparison to QDM corrected data. The differences in SWE and glacier volume transfer to the streamflow components. Especially for the rainfall and snowmelt induced runoff parts the bias correction method leads to significant differences. These differences exceed the variation of the RCMs and can thus be rated with major importance.

After the methods comparison it can be assumed, that the multivariate bias correction method performs better than the univariate quantile mapping. By the nature of its algorithm it includes QDM and additionally preserves the interdependence of the climate variables. This becomes clear in the results: The direct interdependence of the climate variables is better represented in MBCn corrected RCM data. Reference data mostly lie within the range of MBCn corrected RCM data, while QDM corrected data show larger discrepancies. This can be traced througout HBV-light simulations. Streamflow components in the annual mean are significantly closer to observations. QDM underestimates the snowmelt component, partly by 200 mm/yr, and therefore overestimates the rainfall runoff component, while MBCn corrected data largely match observation data. Generally, the variation of RCMs is limited through MBCn and is in better agreement with observed values. In other studies Cannon (2017) also demonstrated better results for MBCn corrected data in comparison to QDM corrected data. However, apart from this, no further study has been found that applied this newly developed method.

Assuming, that the MBCn approach leads to results closer to observations it can be questioned whether results using the well-established univariate quantile mapping approaches lead to precise representations and projections in snow dominated catchments. As shown in this study, especially processes that depend on the interactions of air temperature and precipitation, such as snow fall and accumulation,

glacier melt and the deriving runoff components are strongly influenced by the bias correction method applied. Often the variation introduced by the Euro-CORDEX RCM ensemble is exceeded by the bias correction method.

4.2 Changing trends over the projected time period

Air temperature of all four evaluated alpine catchments is subject to major projected changes under the assumption of the RCP scenarios 4.5 and 8.5. Especially annual mean air temperatures are projected to increase during the 21^{st} century. Gobiet et al. (2014) confirms that this positive trend can be considered as robust projection even though the magnitude is quite uncertain and varies depending on RCMs. Gobiet et al. (2014) furthermore points towards anomalous warming at higher elevations that might be triggered by feedback mechanisms of reduced snow cover and albedo. For the evaluated alpine catchments the scenario RCP 4.5 shows an increase in air temperature of around 2-3 K until 2100, while the non-intervention scenario RCP 8.5 indicates an even higher increase of 4-6 K by the end of the 21^{st} century. Similar ranges were also found by Farinotti et al. (2011) who report a mean air temperature rise between 2.2 K and 5.2 K until the end of the century in comparison to the reference period 1980-2009. This corresponds to an average warming of $+0.4\pm0.1$ K per decade. The older SRES scenarios supposed similar ranges of annual temperature increase (Fischer et al. 2012). Along with increasing air temperatures, the annual regime of the zero-degree-level is shifted upwards (appendix B1). This tendency is also shown by Bavay et al. (2009).

While no significant differences in the annual precipitation amount can be detected, the physical state of precipitation is subject to change. It is simulated that increasing air temperatures lead to a shift from snowfall to rain - a trend that was also decribed by Bavay et al. (2009). The number of days with snowfall is decreasing during the simulation period and, accordingly, an increase in the number of rainy days is simulated. This development is in line with the current assessment of climate change. Farinotti et al. (2011) predicts an increase in liquid precipitation by 15-35%.

The trend of decreasing snowfall highly affects the alpine snow cover (Bavay et al. 2009). As air temperatures get warmer, less precipitation falls as snow and less snow accumulates through the course of a year (Jenicek et al. 2016). Schmucki et al. (2017) confirmed, that the small increase in winter precipitation cannot balance the strong influence of higher air temperatures. While a projected decrease is clear, the magnitude of decrease strongly depends on the RCM and the bias correction method applied and covers a wide range especially towards the end of the 21^{st} century. However, under the more extreme non-intervention RCP 8.5 scenario snow accumulation is reduced by half in comparison to the reference period. It is noticeable that there is a reduction of snow during all the seasons and Bavay et al. (2009) state that the reduction is noted in all elevation zones. Within the recent years the snow cover has already declined (Bavay et al. 2009, Stahl et al. 2016). While the current climate still supports permanent snow cover and ice at high altitudes above 3000 m a.s.l., this zone would shift up and disappear under common future climate scenarios (Bavay et al. 2009). The transition zone between marginal and dominant snow

cover, and therefore the snow line, lies currently above 2000 m a.s.l., what is also claimed by Bavay et al. (2009). Bavay et al. (2009) furthermore concluded that these altitudes are the elevation ranges of the evaluated catchments, that are experiencing the most changes within the 21^{st} century. At lower altitudes below 1200 m a.s.l time-continuous winter snow cover is simulated to become an exception rather than the rule according to Bavay et al. (2009). Furthermore, a change in the duration of the snow cover is noticeable in the simulations, even though, inter-annual variations of the snowmelt peak are extremely pronounced and cover a range of more than a month ranging from late April to early June. On average, the snow free period in the summer is simulated to become longer. An explanation for this is given by Bavay et al. (2009) who showed that the snowfall onset is subject to the timing of the first major precipitation event during freezing temperatures and therefore dependent on a combination of both climate variables. The first storms in fall might therefore fall as rain in the future, as temperatures are expected to rise, and the snow cover starts later in the year. The end of snowmelt, is mainly influenced by air temperatures and the amount of snow accumulated. As less SWE is simulated in the projected time period and spring temperatures are projected to be higher, the melting process lasts shorter and is simulated to finish about one month earlier compared to the reference period. Similar results were found by Jenicek et al. (2016).

Furthermore, a clear decreasing trend in glacier volume was simulated. Apart from the 1970s, where some glaciers in the European Alps were in a rather stable equilibrium (also shown by Stahl et al. (2016)), all glaciers loose in volume until the end of the simulation period in 2100. Over recent decades even an acceleration of the glacier melt has been found all over the European Alps (Vincent et al. 2017). The main driving force of this phenomenon is the lacking stability of glaciers in periods of changing air temperatures. RCM scenarios simulating air temperatures based on the RCP 4.5 and RCP 8.5 emission scenarios indicate air temperature rises of 2-3 K and 4-6 K respectively until the end of the 21^{st} century. In the headwater catchments of the Rhine, many glaciers are already small and show a high sensitivity to rising air temperatures (Huss & Fischer 2016). In this study, glaciers are simulated to shrink quickly and in some catchments even vanish during the simulation period. In the high catchments of the Schwarze and the Weisse Lütschine glacier melt takes a little longer, as the ice volume is larger. Until 2100 about 50-90% of their volume is simulated to be lost for the RCP 4.5 scenario and about 70-100% for the RCP 8.5 scenario. Glaciers at lower elevations in the Hinterrhein or Landquart catchments melt earlier and are simulated to have melted entirely earliest by 2040, latest by the end of the 21^{st} century. These are the catchments in which the glaciers lie in the elevation ranges, in which observed volume changes in small glaciers are the largest according to Fischer et al. (2015). For the small glaciers in these catchments Huss & Fischer (2016) simulated the loss of 90% between 2010 and 2040 and almost all small glaciers are simulated to have melted completely by 2060, except for some glaciers in radiation-protected cirques that additionally are high accumulation areas (Huss & Fischer 2016). Even though glaciers were modelled on the catchment scale and were not differentiated individually, the dimension of the total glacier melt should be realistically represented in the simulated range.

Each of the previously described components of precipitation, snowmelt and

glacier ice melt have their part in the total runoff. With the increasing liquid fraction of precipitation, the runoff part deriving directly from rain increases. This phenomenon is of special importance during autumn and winter. During these seasons in the reference period only a small percentage of precipitation fell as rain, while the rest fell as snow and was stored in a snow layer. A consequence of this development is shown by Bavay et al. (2009), who prognoses a higher probability of flooding, when heavy precipitation events in autumn, that used to fall as snow, are projected to fall as rain. In the same way as the liquid precipitation increases, snow fall decreases. Consequently, less SWE accumulates that can contribute to streamflow, which is also shown by Bavay et al. (2009) and Farinotti et al. (2011). However, the snowmelt runoff part stays relevant in all of the evaluated alpine catchments and will keep contributing to the characteristics of the streamflow regimes. The decrease of the snowmelt runoff part is a clear trend, that is detected for both scenarios using both bias correction methods, yet, the amount of decrease varies. Especially under the RCP 8.5 scenario, the snowmelt component is simulated much smaller and even smaller when the QDM bias correction method was used in comparison to MBCn corrected data as mentioned earlier on. The runoff peak generated by snowmelt is reached during the main snowmelt season in spring with large inter-annual differences in the timing. The streamflow peaks are projected to be narrower and more concentrated under future scenarios and the influence of snowmelt on streamflow ends earlier in the course of a year. Jenicek et al. (2016) illustrated this phenomenon doing detailed studies in correlating summer low flows with the SWE amount during the winter. The inter-annual variation of glacier ice melt runoff is not as pronounced as snowmelt or rain runoff parts. A continuous decrease and final lack of the glacier ice melt runoff component was detected for the Landquart and Hinterrhein catchments, where only a small percentage of glacierized area was left at the beginning of the study period in comparison to 1900. In the catchments with higher glacierization and a higher elevation a trend in glacier runoff could be found. Until 2010 the glacier ice melt runoff component was stable or increased slightly in the Lütschine catchments, before it started decreasing continuously. This phenomenon can be explained through the compensation effect of the decreasing glacier area and an increasing melt rate due to higher air temperatures. As long as glacier areas are large enough, the decreasing area can be compensated through higher melt rates. This is possible only up to a certain size of the glacier. At a certain point, the increasing air temperatures cannot compensate the decreasing glacier area any more and the absolute glacier melt decreases (Stahl et al. 2016). For all, even substantially glacierized catchments, Farinotti et al. (2011) projects the maximum glacier contribution to occur between 2020 and 2050. For very small glaciers, this peak was already crossed between 1997-2004 (Huss & Fischer 2016).

The combination of all three runoff components, the total annual discharge, stays more or less similar. The natural intra-annual range of streamflow covers a wide range of up to 500 mm. RCMs vary within the same range. Within the catchments of major glacierization, such as the Lütschine catchments, a slight decrease in discharge is noticeable in the second half of the 21^{st} century. This is likely caused by the decreasing storage of glacier ice that can melt (Farinotti et al. 2011). There are also major differences in the timing of discharge within the course of a year. Even

though the glacier ice melt runoff component is a rather small percentage of the total discharge only, it is of major importance during the main melt season in late summer, when the snowmelt season is already over and precipitation is usually low. Lacking glacier runoff contribution after the glacier's total vanishing leads to lower discharge during the late summer especially and runoff regimes shift from glacial to nivo-glacial and finally nival regimes (Farinotti et al. 2011, Stahl et al. 2016). Therefore, changes in runoff regimes are more pronounced for catchments with a high degree of glacierization (Farinotti et al. 2011). The snowmelt component is of major importance for the annual runoff in both, past and future. It determines the intra-annual runoff regime. The snowmelt runoff and the precipitation runoff and therefore the total discharge increase during the winter as air temperatures are simulated to increase.

5 Conclusion

In this study a major focus was laid on the correct representation of climate variables and their interdependencies before using them as input for hydrological modelling. Therefore, a lately developed multivariate bias correction method was used to preserve the climate variables' interdependences during the bias correction process. For the comparison with results from other studies, the more common univariate quantile mapping was used as well. Due to the nature of the bias correction algorithms, most differences were found in the interdependence of air temperature and precipitation: MBCn corrected RCM data simulate more snowfall and consequently up to 50% more snow accumulation than QDM corrected RCM data. This is a relevant difference despite variations of the RCM ensemble. Furthermore, similar tendencies are detected when simulating glacier volume. MBCn corrected data always simulate a higher glacier volume than QDM corrected RCM data. Yet, the RCM variation is large and the differences caused by the bias correction methods lie within this range. These distinctions trace into the simulations of streamflow. The snowmelt runoff component is higher for simulations based on MBCn corrected RCM data in comparison to QDM corrected data while the precipitation runoff component behaves the opposite way. The glacier ice melt runoff component is simulated quite stable, as it is mainly dependant on air temperatures rather than the climate variables' interactions. For catchments including the elevation range of the snow line, where the interdependence of air temperature and precipitation is of major importance, it is assumed that multivariate correction methods perform more accurate compared to univariate quantile mapping approaches.

Based on the accurate representation of climate model data, this study's aim was to simulate hydrological conditions under the influence of the prospected climate change in four partly glacierized alpine catchments. The RCM data from the Euro-CORDEX ensemble used in this study indicate an increase in air temperature of 2-3 K (RCP 4.5 scenario) and 4-6 K (RCP 8.5 scenario) respectively by 2100 in comparison to the reference period from 1976-2006. This triggers a change in the composition of precipitation from snowfall to rainfall. As snowfall is limited under future simulations, the snow accumulation diminishes. This becomes apparent in the annually accumulated amount of SWE and in the duration of the snow cover. Depending on RCM and bias correction method, the SWE is simulated to decrease by up to 50%. The snow cover period shortens by partly more than a month due to both, a later onset of snow accumulation and an earlier onset of snowmelt. With rising air temperatures, glaciers also lose their equilibrium and – except for a short period of stability in the 1970s – melt continuously until the end of the simulation period in 2100. In the Hinterrhein and Landquart catchments, glaciers were even simulated to be vanished earliest by 2040, latest by the end of the 21^{st} century, depending on different RCMs and emission scenarios.

These changes naturally have effects on streamflow. The increasing liquid fraction in precipitation leads to higher runoff during fall and winter, where precipitation used to fall as snow that was stored in a snow cover during the reference period. With decreasing SWE and rising air temperatures, the snowmelt runoff component is subject to change. Snowmelt runoff peaks are simulated to become narrower as the snowmelt

lasts shorter. It then loses its influence on the streamflow in summer. However, the snowmelt stays the characterizing runoff component in the highly elevated alpine catchments. While in currently nivo-glacial regimes glacier ice melt is still of major importance, its influence decreases as glaciers are undergoing mass losses. So far, the glacier ice melt runoff contributes to streamflow in late summer preventing low flows in dry years. The total annual runoff stays similar in slightly glacierized catchments, but is slightly decreasing in catchments with high glacier ice melt components as ice storages shrink. The annual runoff regime is however subject to change with higher streamflow during winter, an altered runoff peak in spring and lower runoff during the summer months.

The simulated changes in streamflow are likely to have impacts in the future. The fraction of liquid precipitation is increasing and so is the streamflow component that depends on direct rainfall. Heavy precipitation events in autumn or winter increase the probability of flooding in the future. In the past, and still nowadays, autumn storms mostly go down as snow being stored in a snow layer not leading to direct runoff (Bavay et al. 2009). But more important than the impacts of increasing rainfall are the impacts of the decreasing solid fraction of precipitation. The shorter duration of the snow cover and the melting period, as well as the decrease in SWE, are likely to affect soil and groundwater storages. Especially during the melting season in spring, soil and groundwater storages are recharged by meltwater (Jenicek et al. 2016). Furthermore, low flows in summer are influenced by the SWE of the previous winter. A lower SWE leads to earlier occurring low flows during the summer and favours droughts in times of little rain. This process is influenced directly through smaller availability of SWE meltwater, but also indirectly, as the groundwater recharge and consequently the catchment's baseflow is lower (Jenicek et al. 2016). Moreover, as the loss in glacier volume can no longer be compensated and the glacier ice meltwater components decrease, the ecosystem services that the glaciers supply, such as the cooling effect on microclimate on the areas surrounding the glacier, will no longer be provided. The lack of this cooling effect can lead to feedback mechanisms such as anomalous warming in high elevations. Moreover, winter tourism in the Swiss Alps relies on the presence of glacier remnants and snow accumulation (Schmucki et al. 2017). The runoff from glacier storages, especially during the projected warmer and drier summers in Central Europe, will be missing during low flows in summer. Especially in dry summers, as in 1921, 1947 or 2003, it used to be an important component in the Rhine's discharge balancing low flows. Droughts during the late summer might therefore intensify in the future (Stahl et al. 2016). Water resource management needs to be adapted to less water availability during dry summer months, especially in dry inner alpine valleys. While groundwater levels are likely to be sinking, irrigation might become limited. Furthermore, hydropower generation and shipping need to be adapted to the changing water availability (Huss 2011).

In this study it is shown that different bias correction methods can lead to significantly different results. Especially in catchments that are crossed by the snow line, the correct representation of the interdependence of air temperature and precipitation plays a crucial role in hydrological modelling. This study can therefore be regarded as a strong argument towards the consideration of using multivariate

bias correction methods in climate change impact studies in the hydrological field. It furthermore shows the entity of hydrological processes in high alpine catchments under projected climate conditions in the 21^{st} century.

For further research it would be interesting to conduct the study, that in this case was done in four exemplary catchments, for the entire Rhine basin. It would allow assessing alterations in streamflow due to changing climate conditions on a larger scale and further downstream. On the technical site, more studies comparing bias correction methods could help supporting the results of better performing multivariate bias correction algorithms found in this case.

References

Bavay, M., Lehning, M., Jonas, T. & Löwe, H. (2009), 'Simulations of future snow cover and discharge in Alpine headwater catchments', *Hydrological Processes* **23**, 95–108. doi: 10.1002/hyp.7195.

Blanc, P. & Schädler, B. (2013), 'Das Wasser in der Schweiz: Ein Überblick', *Schweizerische Hydrologische Kommission (CHy), Bern* pp. 1–28. ISBN: 978-3-9524235-0-9.

Bürger, G., Schulla, J. & Werner, A. T. (2011), 'Estimates of future flow, including extremes, of the Columbia River headwaters', *Water Resources Research* **47**(W10520), 1–18. doi: 10.1029/2010WR009716.

Cannon, A. (2016*a*), 'Multivariate Bias Correctin of Climate Model Outputs', *R: a language and environment for statistical computing* **0.10-1**. R foundation for Statistical Computing, Vienna. http://CRAN.R-project.org/package=MBC.

Cannon, A. (2016*b*), 'Multivariate Bias Correction of Climate Model Output: Matching Marginal Distributions and Intervariable Dependence Structure', *Journal of Climate* **29**, 7045–7064. doi: 10.1175/JCLI-D-15-0679.1.

Cannon, A. (2017), 'Multivariate quantile mapping bias correction: an N-dimensional probability density function transform for climate model simulations of multiple variables', *Climate Dynamics* pp. 1–19. doi: 10.1007/s00382-017-3580-6.

Cannon, A., Sobie, S. R. & Murdock, T. Q. (2015), 'Bias Correction of GCM Precipitation by Quantile Mapping: How Well do Methods Preserve Changes in Quantiles and Extremes?', *Journal of Climate* **28**, 6938–6959. doi: 10.1175/JCLI-D-14-00754.1.

Clark, M., Gengopadhyay, S., Hay, L., Rajagopalan, B. & Wilby, R. (2004), 'The Schaake shuffle: A method for reconstructing space–time variability in forecasted precipitation and temperature fields', *Journal of Hydrometeorology* **5**, 243–262. doi: 10.1175/1525-7541(2004)005,0243:TSSAMF.2.0.CO;2.

Ehret, U., Zehe, E., Wulfmeyer, V., Warrach-Sagi, K. & Liebert, J. (2012), 'Should we apply bias correction to global and regional climate model data?', *Hydrology and Earth System Sciences* **16**, 3391–3404. doi: 10.5194/hess-16-3391-2012.

Farinotti, D., Usselmann, S., Huss, M., Bauder, A. & Funk, M. (2011), 'Runoff evolution in the Swiss Alps: projections for selected high-alpine catchments based on ENSEMBLES scenarios', *Hydrological Processes* **25**, 1–16. doi: 10.1002/hyp.8276.

Fischer, A. M., Weigel, A. P., Buser, C. M., Knutti, R., Künsch, H. R., Liniger, M. A., Schär, C. & Appenzeller, C. (2012), 'Climate change projections for Switzerland based on a Bayesian multi-model approach', *International Journal of Climatology* **32**, 2348–2371. doi: 10.1002/joc.3396.

Fischer, M., Huss, M., Barboux, C. & Hoelzle, M. (2014), 'The new Swiss Glacier Inventory SGI2010: relevance of using high-resolution source data in areas dominated by very small glaciers', *Arctic, Antarctic and Alpine Research* **46**(4), 933–945. doi: 10.1657/1938-4246-46.4.933.

Fischer, M., Huss, M. & Hoelzle, M. (2015), 'Surface elevation and mass changes of all Swiss glaciers 1980-2010', *The Cryosphere* **9**, 525–540. doi: 10.5194/tc-9-525-2015.

FOEN (Federal Office for the Environment) (2010), 'Hydrologischer Atlas der Schweiz (HADES)'. http://hydrologischeratlas.ch/de [28.08.2017].

FOEN (Federal Office of Meteorology and Climatology, MeteoSwiss) (2014), 'Climate of Switzerland'. http://www.meteoswiss.admin.ch/home/climate/past/climate-of-switzerland.html [27.04.2017].

Freudiger, D., Kohn, I., Seibert, J., Stahl, K. & Weiler, M. (2017), 'Snow redistribution for the hydrological modeling of alpine catchments', *Wiley Interdisciplinary Reviews: Water* **4**(5), 1–16. doi: 10.1002/wat2.1232.

Glaciological Reports (1958/59-2010/11), 'The Swiss Glaciers', *Yearbooks of the Cryospheric Commission of the Swiss Academy and Sciences (SCNAT), Laboratory of Hydraulics, Hydrology and Glaciology (VAW) of ETH Zürich, Zürich (Switzerland)* **80-132**.

Gobiet, A., Kotlarski, S., Beniston, M., Heinrich, G., Rajczak, J. & Stoffel, M. (2014), '21st century climate change in the European Alps - A review', *Science of the Total Environment* **493**, 1138–1151. doi: 10.1016/j.scitotenv.2013.07.050.

Hänggi, P. & Weingartner, R. (2011), 'Inter-annual variability of runoff and climate within the Upper Rhine River basin, 1808-2007', *Hydrological Sciences Journal* **56**(1), 34–50. doi: 10.1080/02626667.2010.536549.

Huss, M. (2011), 'Present and future contribution of glacier storage change to runoff from macroscale drainage basins in Europe', *Water Resources Research* **47**(W07511), 1–14. doi: 10.1029/2010WR010299.

Huss, M., Farinotti, D., Bauder, A. & Funk, M. (2008), 'Modelling runoff from highly glacierized alpine drainage basins in a changing climate', *Hydrological Processes* **22**(19), 3888–3902. doi: 10.1002/hyp.7055.

Huss, M. & Fischer, M. (2016), 'Sensitivity of Very Small Glaciers in the Swiss Alps to Future Climate Change', *Frontiers in Earth Science* **4**(34), 1–17. doi: 10.3389/feart.2010.00034.

Huss, M., Jouvet, G., Farinotti, D. & Bauder, A. (2010), 'Future high-mountain hydrology: a new parametrization of glacier retreat', *Hydrology and Earth System Sciences* **14**, 815–829. doi: 10.5194/hess-14-815-2010.

IPCC (2013), 'Climate Change', *The Physical Science Basis, Working Group I Contribution to the Fifth Assessment Report of the Intergovernmental Panel on Climate Change, WMO/UNEP, Cambridge University Press, Geneva (CH)* .

Jenicek, M., Seibert, J., Zappa, M., Staudinger, M. & Jonas, T. (2016), 'Importance of maximum snow accumulation for summer low flows in humid catchments', *Hydrology and Earth System Sciences* **20**, 859–874. doi:10.5194/hess-20-859-2016.

Johnson, F. & Sharma, A. (2012), 'A nesting model for bias correction of variability at multiple time scales in general circulation model precipitation simulations', *Water Resources Research* **48**(W01504), 1–16. doi: 10.1029/2011WR010464.

Köplin, N., Viviroli, D., Schädler, B. & Weingartner, R. (2010), 'How does climate change affect mesoscale catchments in Switzerland? - a framework for a comprehensive assessment', *Advances in Geosciences* **27**, 111–119. doi: 10.5194/adgeo-27-111-2010.

Li, H., Sheffield, J. & Wood, E. F. (2010), 'Bias correction of monthly precipitation and temperature fields from intergovernmental Panel on Climate Change AR4 models using equidistant quantile matching', *Journal of Geophysical Research* **115**(D10101), 1–20. doi: 10.1029/2009JD012882.

Maraun, D. (2016), 'Bias Correcting Climate Change Simulations - a Critical Review', *Current Climate Change Reports* **2**, 211–220. doi: 10.1007/s40641-016-0050-x.

Mehrotra, R. & Sharma, A. (2012), 'An improved standardization procedure to remove systematic low frequency variability biases in GCM simulations', *Water Resources Research* **48**(W12601), 1–8. doi: 10.1029/2012WR012446.

Mehrotra, R. & Sharma, A. (2016), 'A Multivariate Quantile-Matching Bias Correction Approach with Auto- and Cross-Dependence across Multiple Time Scales: Implicationd for Downscaling', *Journal of Climate* **29**, 3519–3538. doi: 10.11175/JCLI-D-15-0356.1.

Meinshausen, M., Smith, S. J., Calvin, K., Daniel, J. S., Kainuma, M. L. T., Lamarque, J.-F., Matsumoto, K., Montzka, S. A., Raper, S. C. B., Riahi, K., Thomson, A., Velders, G. J. M. & van Vuuren, D. P. (2011), 'The RCP greenhouse gas concentrations and their extensions from 1765 to 2300', *Climatic Change* **109**, 213–241. doi: 10.1007/s10584-011-0156-z.

Müller, F., Caflish, T. & Müller, G. (1976), 'Firn und Eis der Schweizer Alpen, Gletscherinventar', *Vdf Hochschulverlag, ETH Zürich, Zürich* .

Oudin, L., Hervieu, F., Michel, C., Perrin, C., Andréassian, V., Anctil, F. & Loumagne, C. (2005), 'Which potential evapotranspiration input for a lumped rainfall-runoff model? Part 2 - Towards a simple and efficient potential evapotranspiration model for rainfall-runoff modelling', *Journal of Hydrology* **303**, 290–306. doi: 10.1016/j.jhydrol.2004.08.026.

Paul, F., Frey, H. & Le Bris, R. (2011), 'A new glacier inventory for the European Alps from Landsat TM scenes of 2003: Challenges and results', *Annals of Glaciology* **59**, 144–152. 52.

Pellicciotti, F., Bauder, A. & Parola, M. (2010), 'Effect of glaciers on streamflow trends in the Swiss Alps', *Water Resources Research* **46**(W10522), 1–16. doi: 10.1029/2009WR009039.

Scherrer, S. C., Appenzeller, C. & Liniger, M. A. (2006), 'Temperature trends in Switzerland and Europe: Implications for climate normals', *International Journal of Climatology* **26**, 565–580. doi: 10.1002/joc.1270.

Schmucki, E., Marty, C., Fierz, C., Weingartner, R. & Lehnung, M. (2017), 'Impact of climate change in Switzerland on socioeconomic snow indices', *Theoretical and Applied Climatology* **127**, 875–889. doi: 10.1007/s00704-015-1676-7.

Seibert, J. & Vis, M. J. P. (2012), 'Teaching hydrological modeling with a user-friendly catchment-runoff-model software package', *Hydrology and Earth System Sciences* **16**, 3315–3325. doi: 10.5194/hess-16-3315-2012.

Seibert, J., Vis, M. J. P., Kohn, I., Weiler, M. & Stahl, K. (2017), 'Technical Note: Representing glacier dynamics in a semi-distributed hydrological model', *Hydrology and Earth System Sciences* pp. 1–20. doi: 10.5194/hess-2017-158. In review.

Sevruk, B. (1989), 'Reliability of precipitation measurement', *In: Precipitation measurements: WMO/IAHS/ETH Workshop on Precipitation Measurements* (ETH Zürich). 3.-7. December 1989.

Sippel, S., Otto, F. E. L., Forkel, M., Allen, M. R., Guillod, B. P., Heimann, M., Reichstein, M., Seneviratne, S. I., Thonicke, K. & Mahecha, M. D. (2016), 'A novel bias correction methodology for climate impact simulations', *Earth System Dynamics* **7**, 71–88. doi: 10.5194/esd-7-71-2016.

Stahl, K., Moore, R. D., Shea, J. M., Hutchinson, D. & Cannon, A. J. (2008), 'Coupled modelling of glacier and streamflow response to future climate scenarios', *Water Resources Research* **44**(W02422), 1–13. doi: 10.1029/2007WR005956.

Stahl, K., Weiler, M., Freudiger, D., Kohn, I., Seibert, J., Vis, M., Gerlinger, K. & Böhm, M. (2016), 'Abflussanteile aus Schnee- und Gletscherschmelze im Rhein und seinen Zuflüssen vor dem Hintergrund des Klimawandels', *Abschlussbericht an die Internationale Kommission für die Hydrologie des Rheingebiets (KHR)* pp. 1–151.

Teutschbein, C.; Seibert, J. (2010), 'Regional Climate Models for Hydrological Impact Studies at the Catchment Scale: A Review of Recent Modeling Strategies', *Geography Compass* **4**(7), 834–860. doi: 10.1111/j.1749-8198.2010.00357.x.

van Vuuren, D. P., Edmonds, J., Kainuma, M., Riahi, K., Thomson, A., Hibbard, K., Hurtt, G. C., Kram, T., Krey, V., Lamarque, J.-F., Masui, T., Meinshausen, M., Nakicenovic, N., Smith, S. J. & Rose, S. K. (2011), 'The representative concentration pathways: an overview', *Climatic Change* **109**, 5–31. doi: 10.1007/s10584-011-0148-z.

Vincent, C., Fischer, A., Mayer, C., Bauder, A., Galos, S. P., Funk, M., Thibert, E., D., S., Braun, L. & Huss, M. (2017), 'Common climatic signal from glaciers in the European Alps over the last 50 years', *Geophysical Research Letters* **44**, 1376–1383. doi: 10.1002/2016GL072094.

Vrac, M. & Friedrichs, P. (2014), 'Multivariate - Intervariable, Spatial, and Temporal - Bias Correction', *Journal of Climate* **28**, 218–237. doi: 10.1175/JCLI-D-14-00059.1.

Weingartner, R. & Schädler, B. (2001), 'Komponenten des natürlichen Wasserhaushalts 1961-1990)', *Hydrologischer Atlas der Schweiz (HADES)* (Bern). Tafel 6.3.

World Climate Research Programme (WCRP) (2015), 'CORDEX'. http://www.cordex.org/ ; http://www.euro-cordex.net/ [30.04.2017].

Zappa, M. & Kan, C. (2007), 'Extreme heat and runoff extremes in the Swiss Alps', *Natural Hazards Earth System Sciences* **7**, 375–389. doi: 10.5194/nhess-7-375-2007,2007.

Zemp, M., Paul, F., Hoelzle, M. & Haeberli, W. (2008), 'Glacier fluctuations in the European Alps 1850-2000: an overview and spatiotemporal analysis of available data', *The darkening peaks: Glacial retreat in scientific and social context, edited by: Orlove, B., Wiegandt, E. and Luckman, B. H., University of California Press* pp. 152–167.

Zubler, E., Scherrer, S., Croci-Maspoli, M., Liniger, M. & Appenzeller, C. (2014), 'Key climate indices in Switzerland; expected changes in a future climate', *Climate Change* **123**, 255–271. doi: 10.1007/s10584-013-1041-8.

Appendix

List of Figures in Appendix

List of Tables in Appendix

A HBV-light parameters

Parameter	Unit	Explanation
Snow Routine		
T_T	°C	threshold temperature
C_{FMAX}	mm °C^{-1} d^{-1}	degree-day factor
SP	-	seasonal variability in degree-day-factor
SFCF	-	snowfall correction factor
C_{FR}	-	refreezing coefficient
C_{WH}	-	water hold coefficient
$CF_{Glacier}$	-	correction factor glacier
CF_{Slope}	-	correction factor slope
Soil and Evaporation Routine		
FC	mm	max. soil moisture storage
LP	mm	soil moisture value above which ET_{akt}=ET_{pot}
BETA	-	parameter that determines the relative contribution to runoff from rain or snowmelt
Glacier Routine		
KSI	Δt^{-1}	snow to ice conversion factor
KG_{min}	t^{-1}	min. outflow coefficient
d_{KG}	t^{-1}	max. range of outflow coefficient
A_G	mm^{-1}	calibration parameter
Response Function		
α	-	non-linearity coefficient
PERC	mm/Δt	threshold parameter
K_1	d^{-1}	recession coefficient SUZ
K_2	d^{-1}	recession coefficient SLZ
Routing Routine		
MAXBAS	d	redistribution of runoff over time

Table A1: Model parameter HBV-light (HBV-light, Help).

B Results bias correction

Bias correction results are represented for all four evaluated catchments in the same way as in the results chapter 3, where graphs are explained in detail.

B1 Zero-degree-level

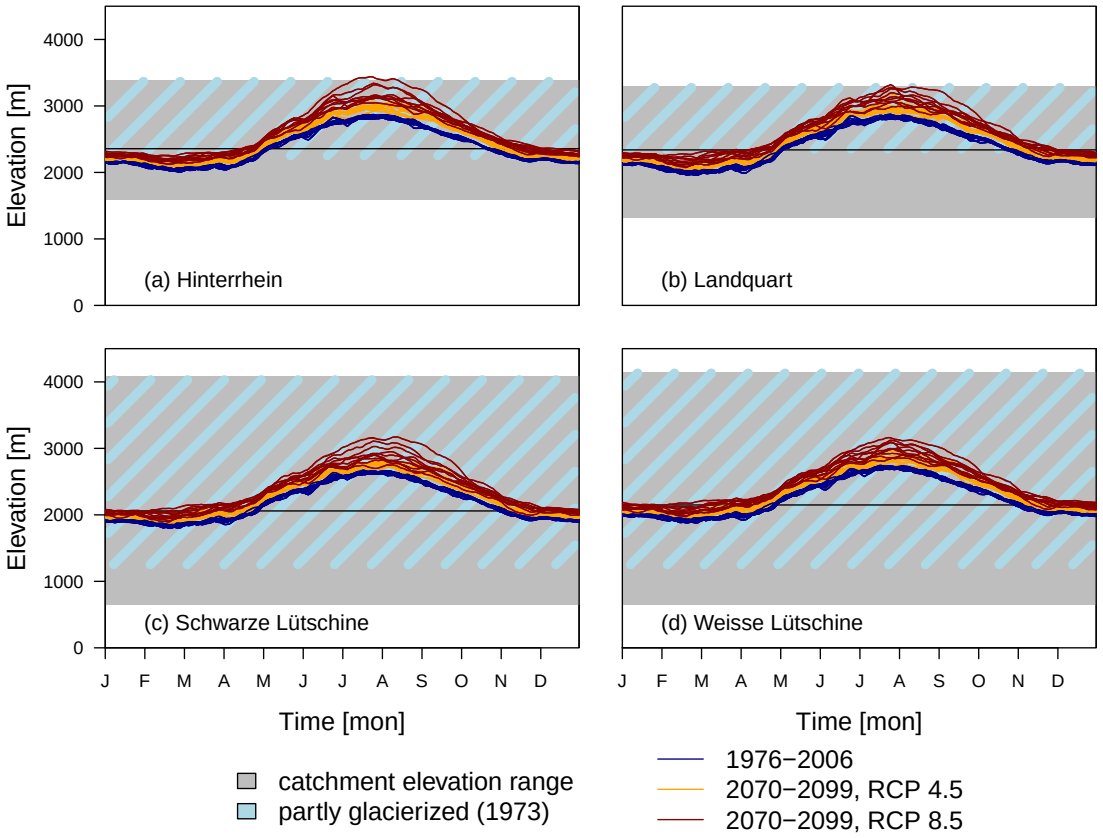

Figure A1: Annual regime of the zero degree level calculated from the range of the RCM ensemble.

B2 Precipitation in dependency on air temperature

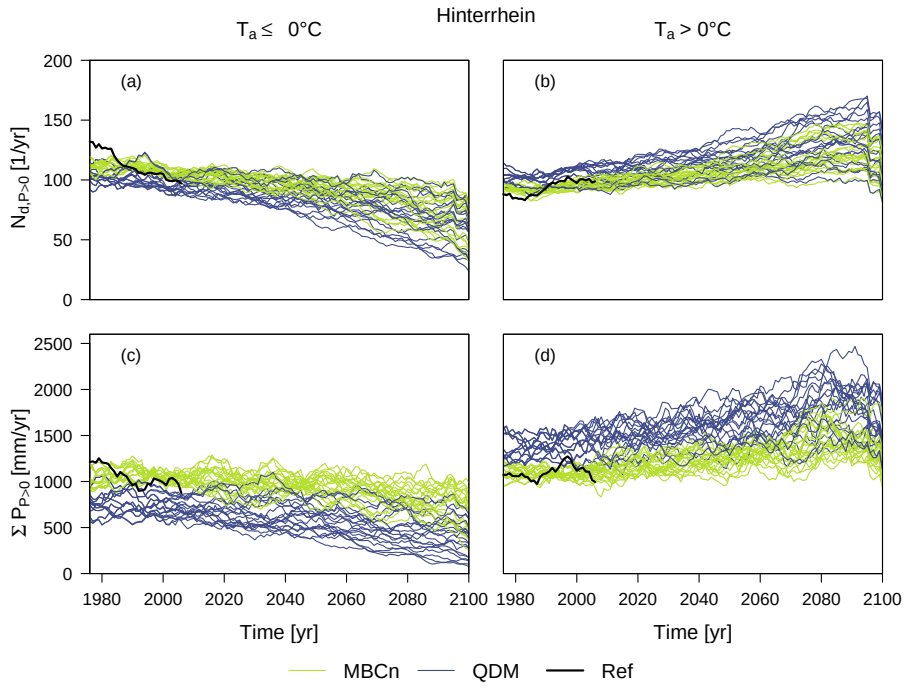

Figure A2: 11-year moving average of the annual number of days with precipitation (P [N_d/yr]) and annual precipitation amounts (P [mm/yr]) (Hinterrhein).

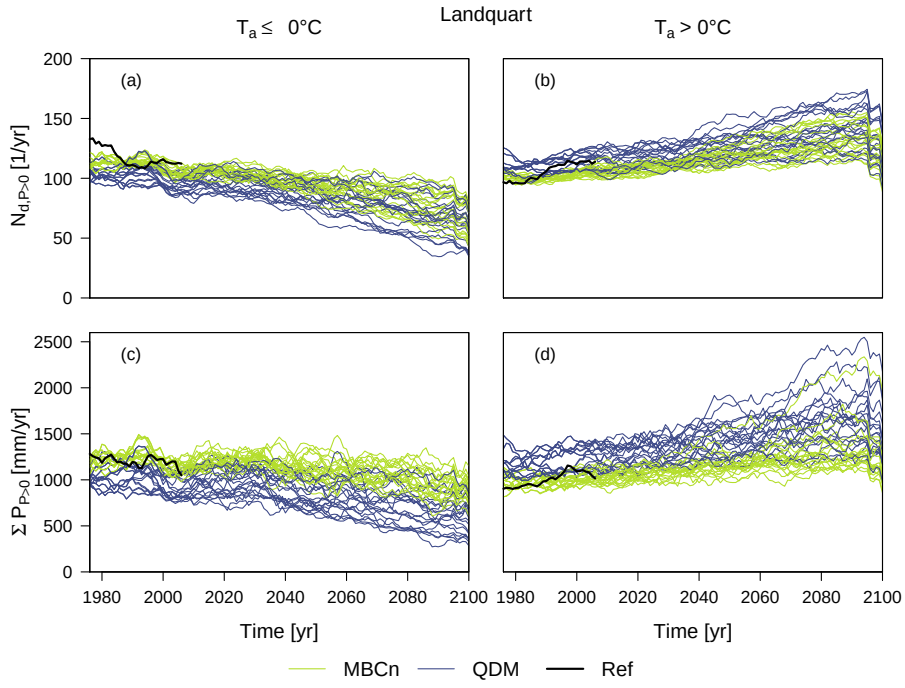

Figure A3: 11-year moving average of the annual number of days with precipitation (P [N_d/yr]) and annual precipitation amounts (P [mm/yr]) (Landquart).

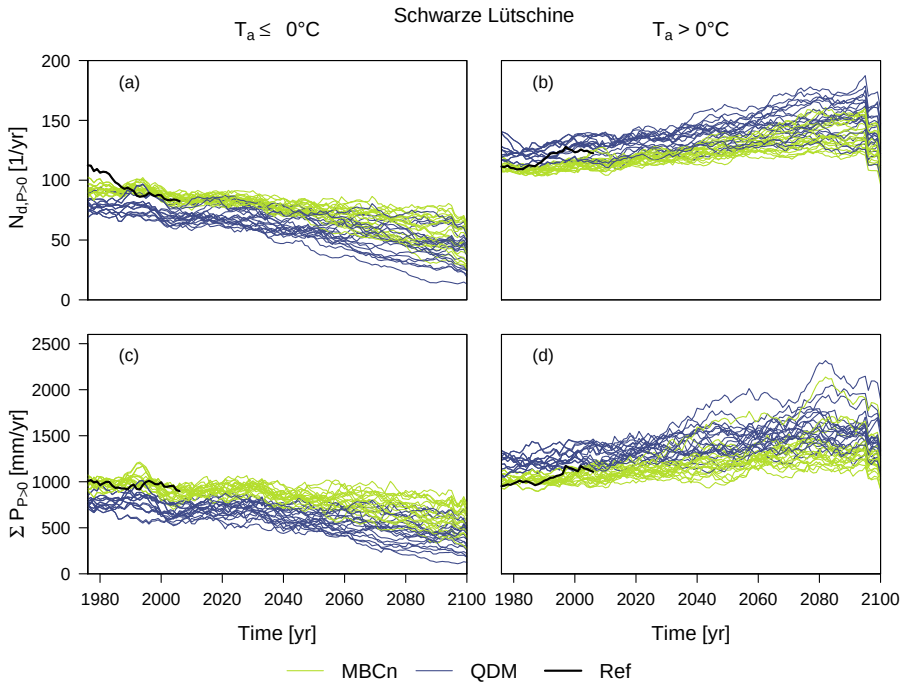

Figure A4: 11-year moving average of the annual number of days with precipitation (P [N_d/yr]) and annual precipitation amounts (P [mm/yr]) (Schwarze Lütschine).

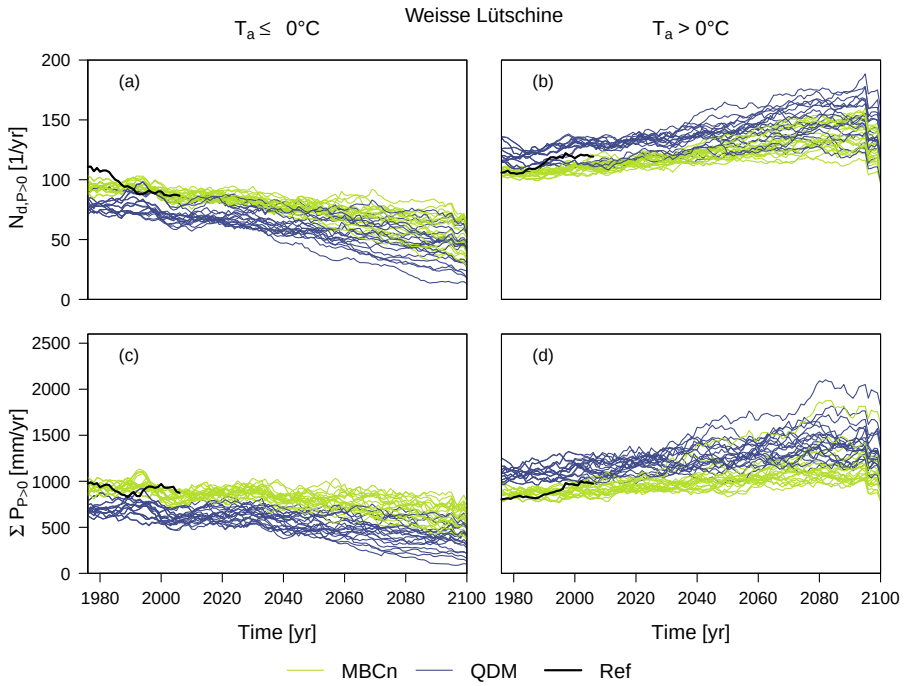

Figure A5: 11-year moving average of the annual number of days with precipitation (P [N_d/yr]) and annual precipitation amounts (P [mm/yr]) (Weisse Lütschine).

B3 Air temperature on dry days

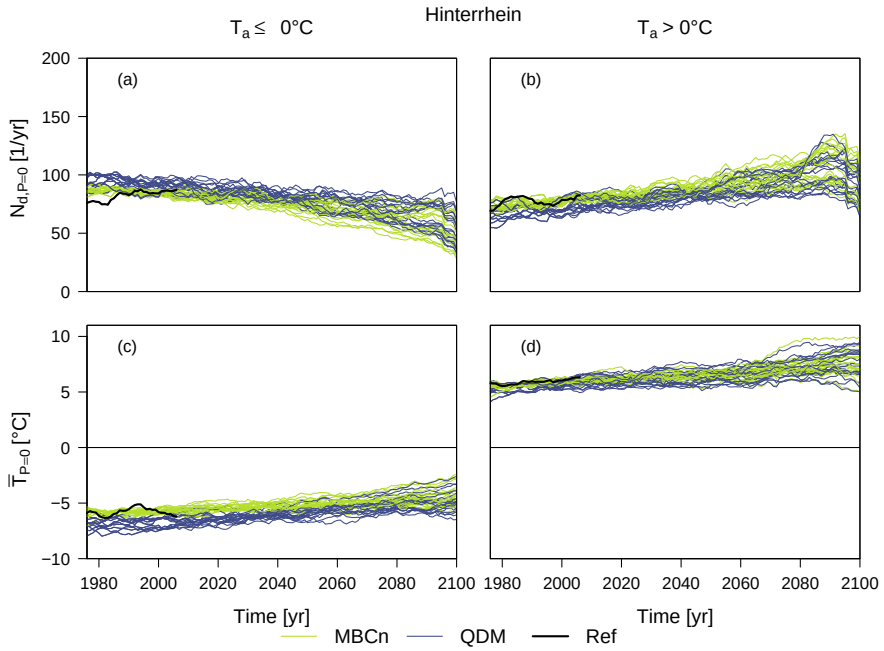

Figure A6: 11-year moving average of the annual number of days without precipitation ($N_{d,P=0mm,T\leq/>0°C}$ [1/yr]) as well as the annual mean temperatures on days without precipitation ($\bar{T}_{P=0mm,T\leq/>0°C}$ [mm/yr]) (Hinterrhein).

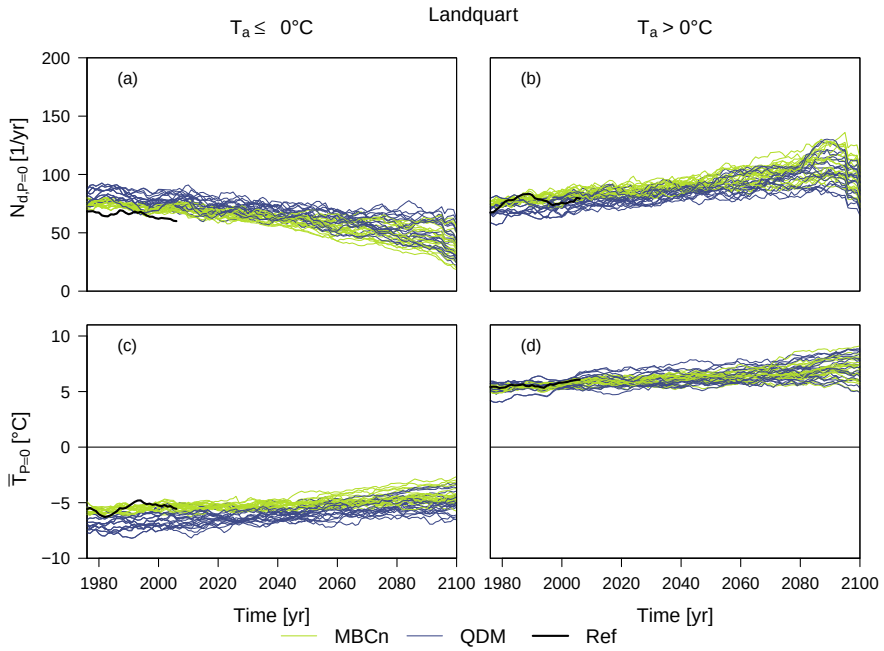

Figure A7: 11-year moving average of the annual number of days without precipitation ($N_{d,P=0mm,T\leq/>0°C}$ [1/yr]) as well as the annual mean temperatures on days without precipitation ($\bar{T}_{P=0mm,T\leq/>0°C}$ [mm/yr]) (Landquart).

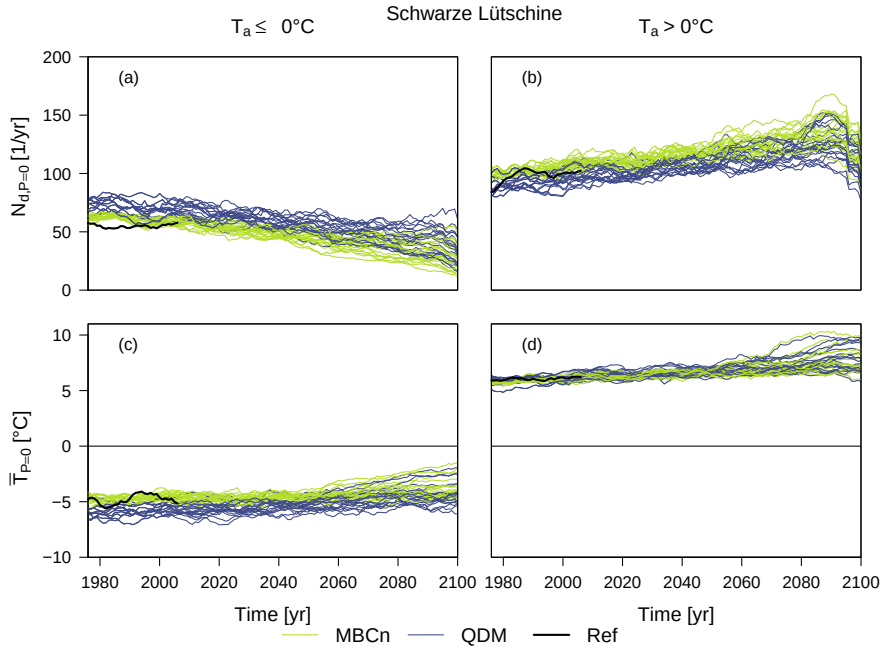

Figure A8: 11-year moving average of the annual number of days without precipitation ($N_{d,P=0mm,T\leq/>0°C}$ [1/yr]) as well as the annual mean temperatures on days without precipitation ($\bar{T}_{P=0mm,T\leq/>0°C}$ [mm/yr]) (Schwarze Lütschine).

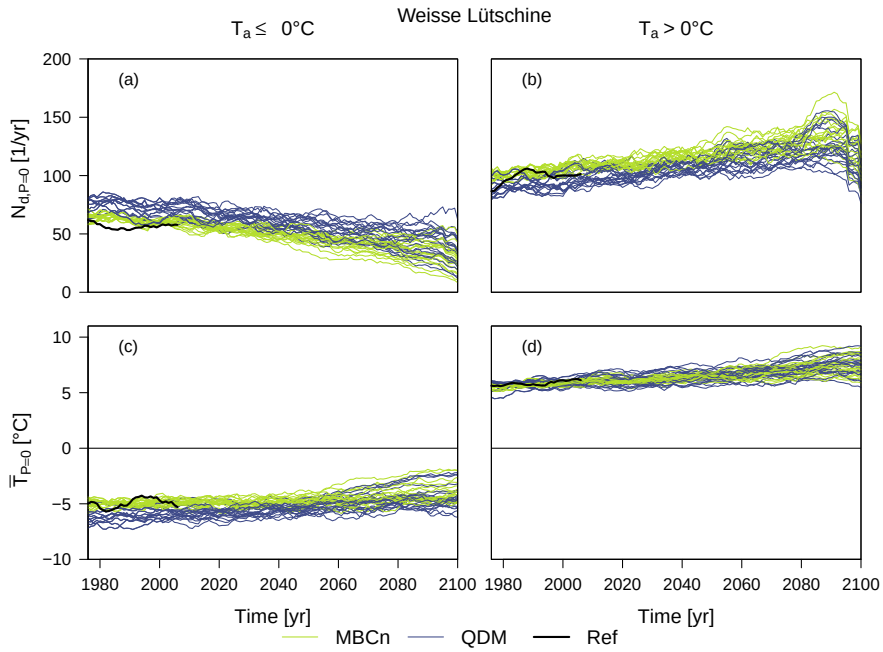

Figure A9: 11-year moving average of the annual number of days without precipitation ($N_{d,P=0mm,T\leq/>0°C}$ [1/yr]) as well as the annual mean temperatures on days without precipitation ($\bar{T}_{P=0mm,T\leq/>0°C}$ [mm/yr]) (Weisse Lütschine).

C Results HBV-light simulations

C1 Snow water equivalent

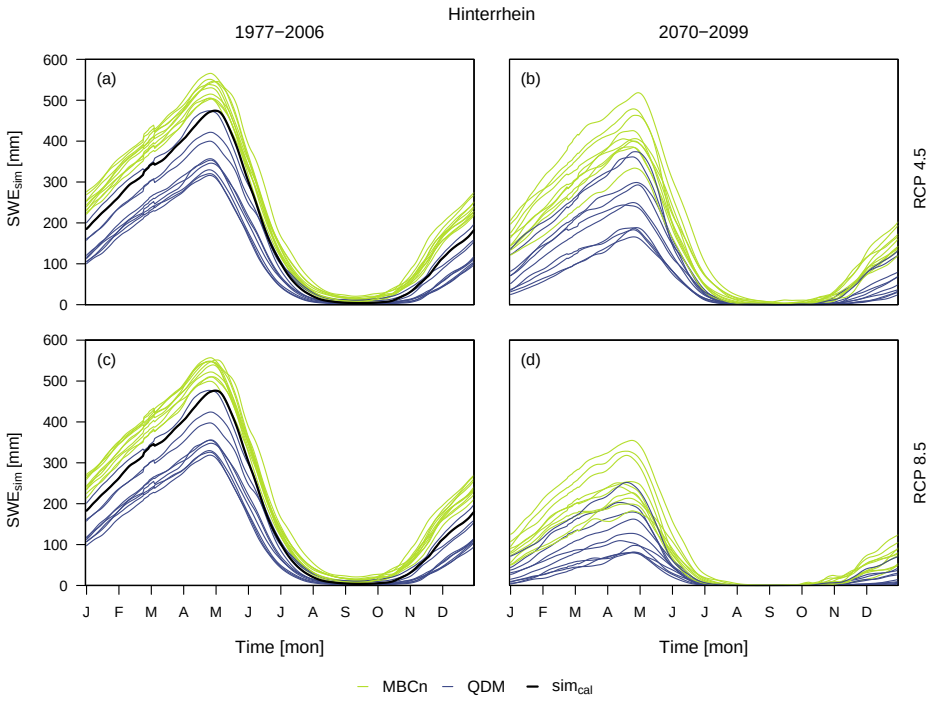

Figure A10: 11-day moving average of the annual SWE (Hinterrhein).

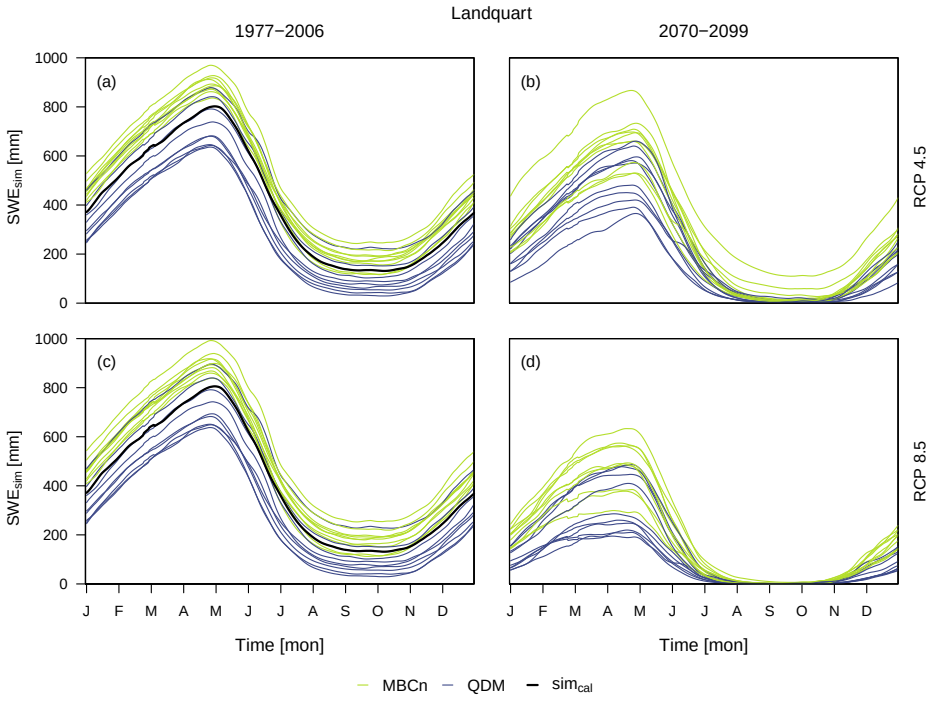

Figure A11: 11-day moving average of the annual SWE (Landquart).

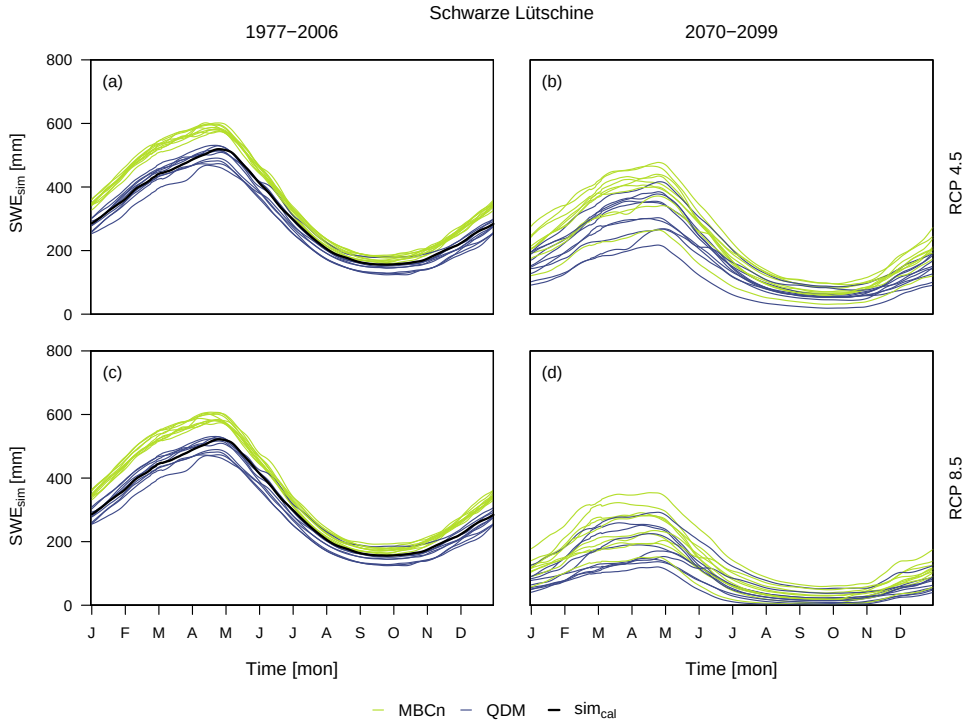

Figure A12: 11-day moving average of the annual SWE (Schwarze Lütschine).

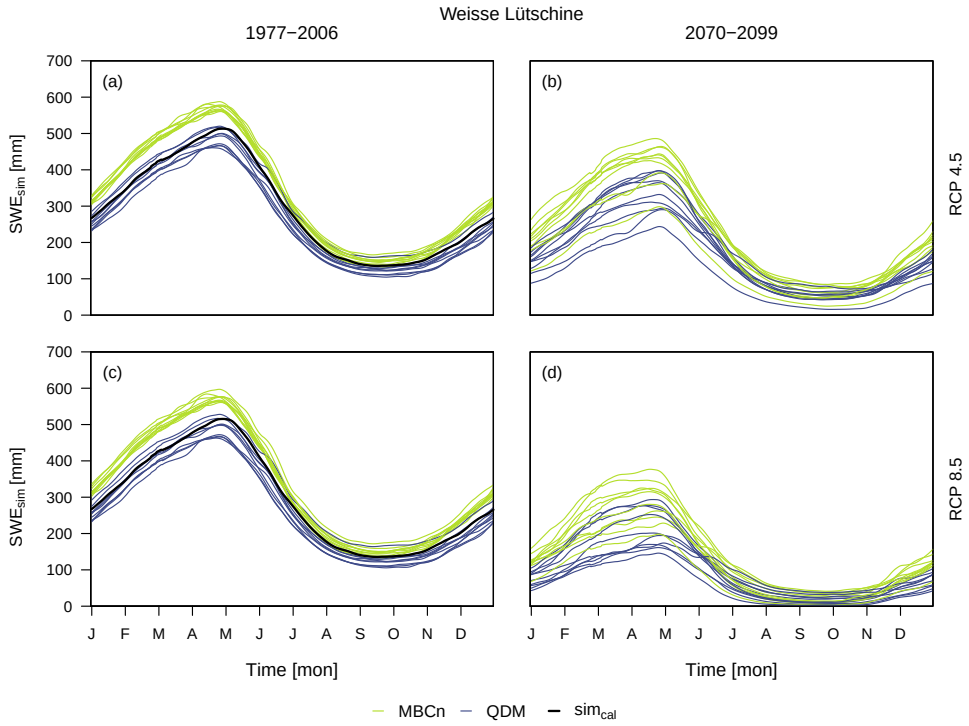

Figure A13: 11-day moving average of the annual SWE (Weisse Lütschine).

C2 Mean annual streamflow

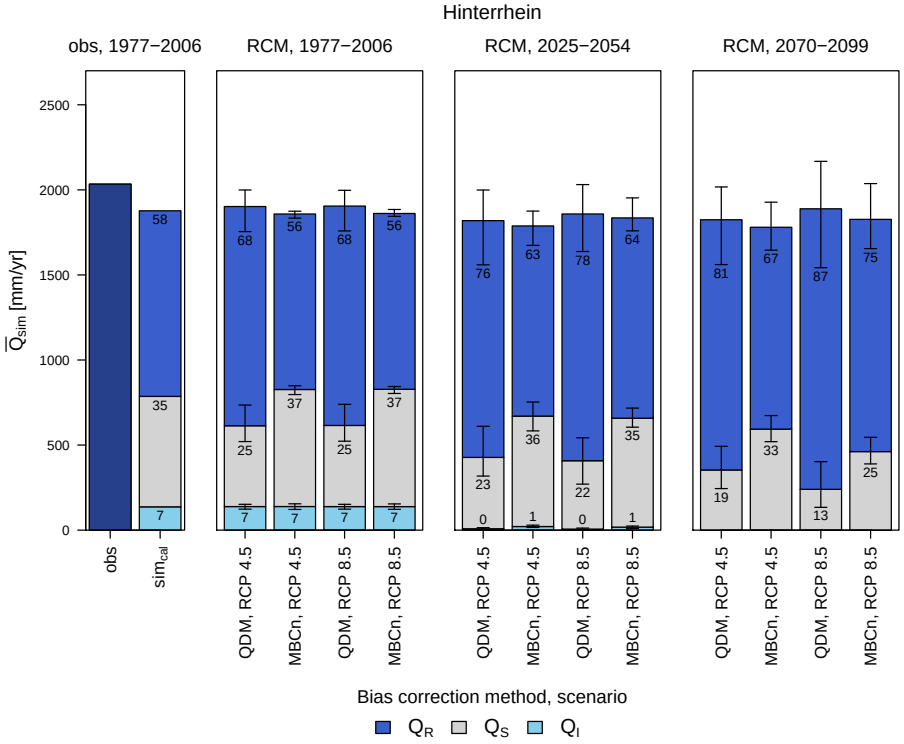

Figure A14: Mean annual runoff sums (Hinterrhein).

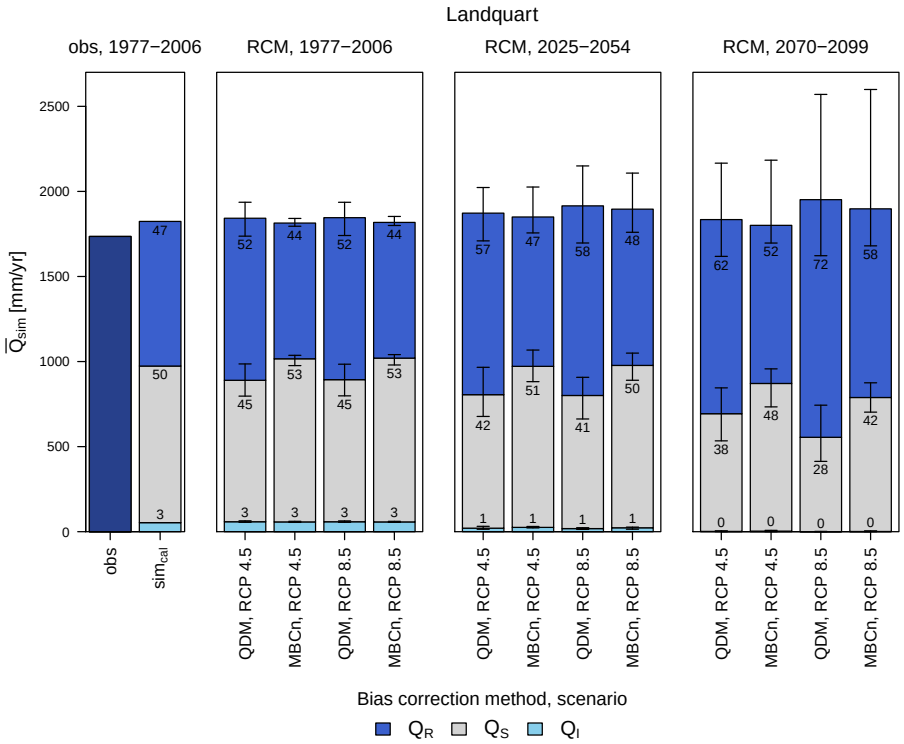

Figure A15: Mean annual runoff sums (Landquart).

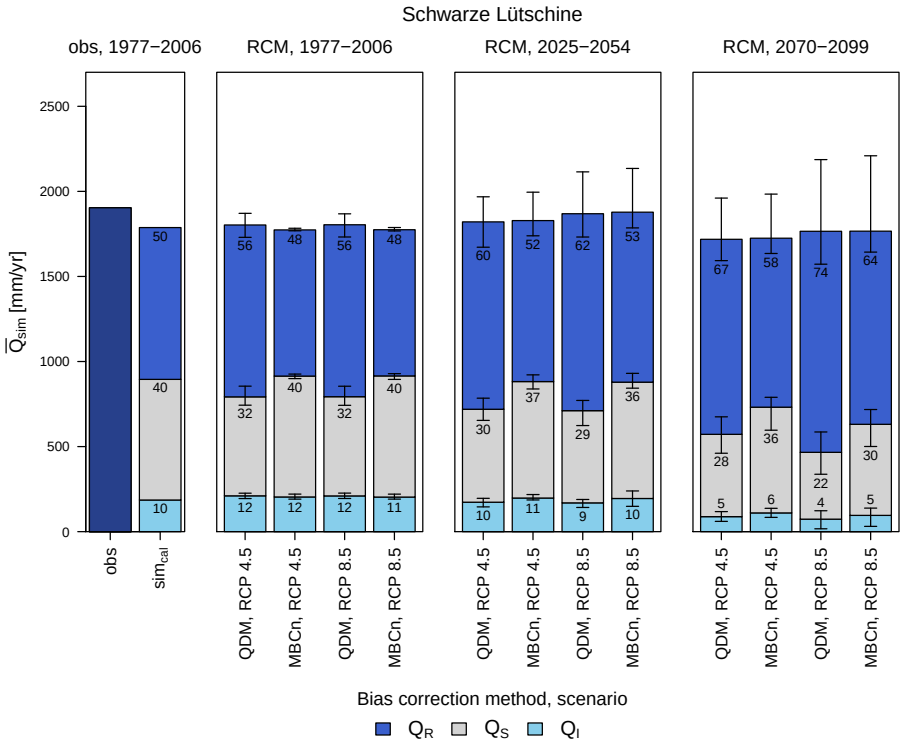

Figure A16: Mean annual runoff sums (Schwarze Lütschine).

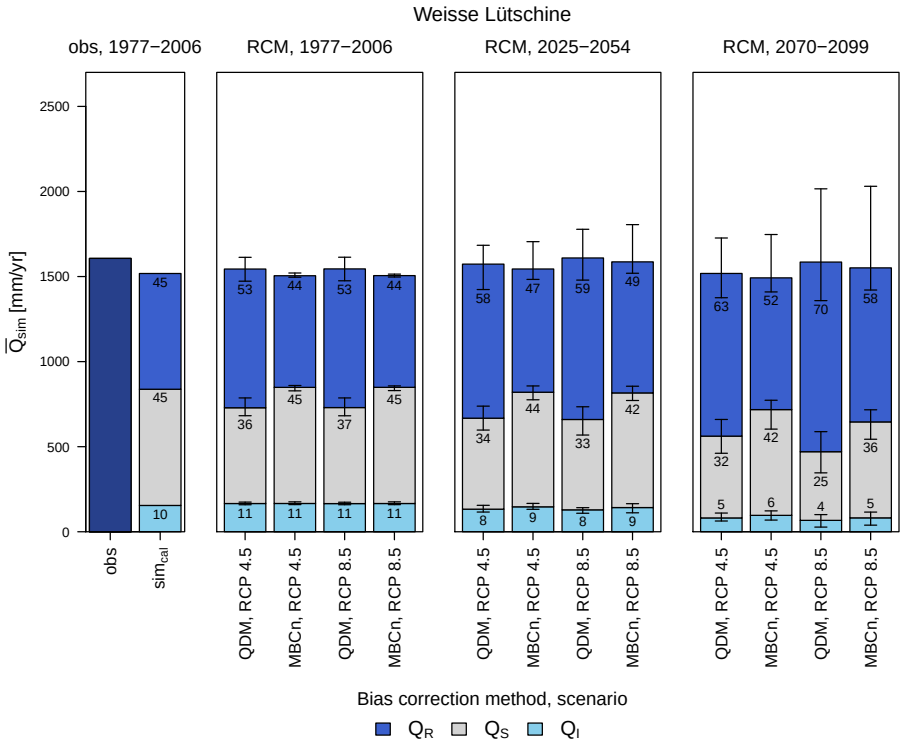

Figure A17: Mean annual runoff sums (Weisse Lütschine).

C3 Time series mean annual streamflow

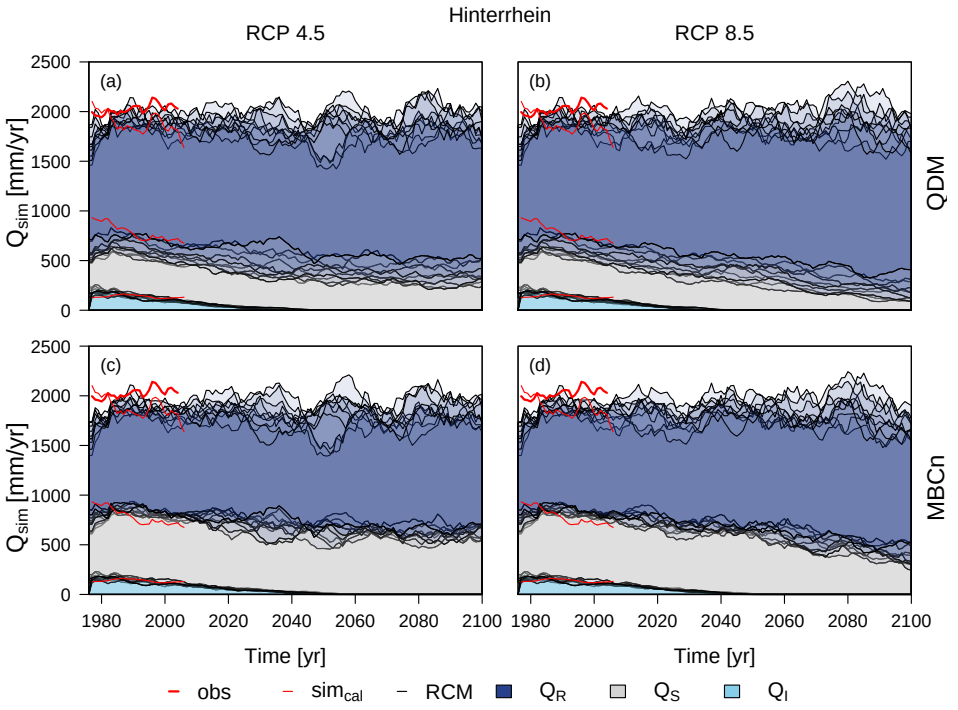

Figure A18: 11-year moving average of annual runoff sums (Hinterrhein).

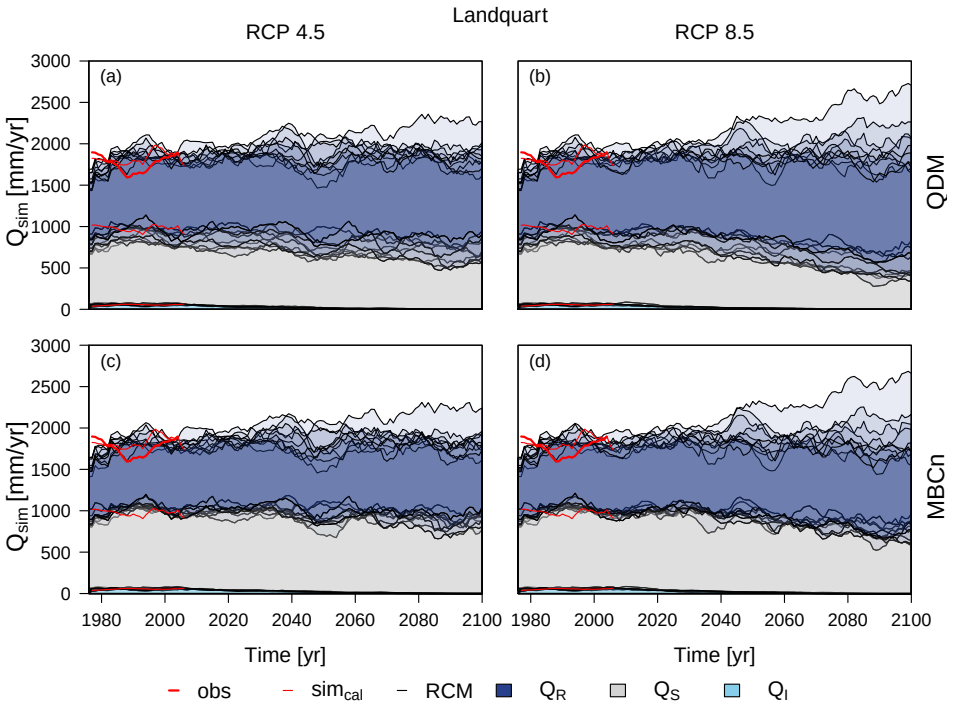

Figure A19: 11-year moving average of annual runoff sums (Landquart).

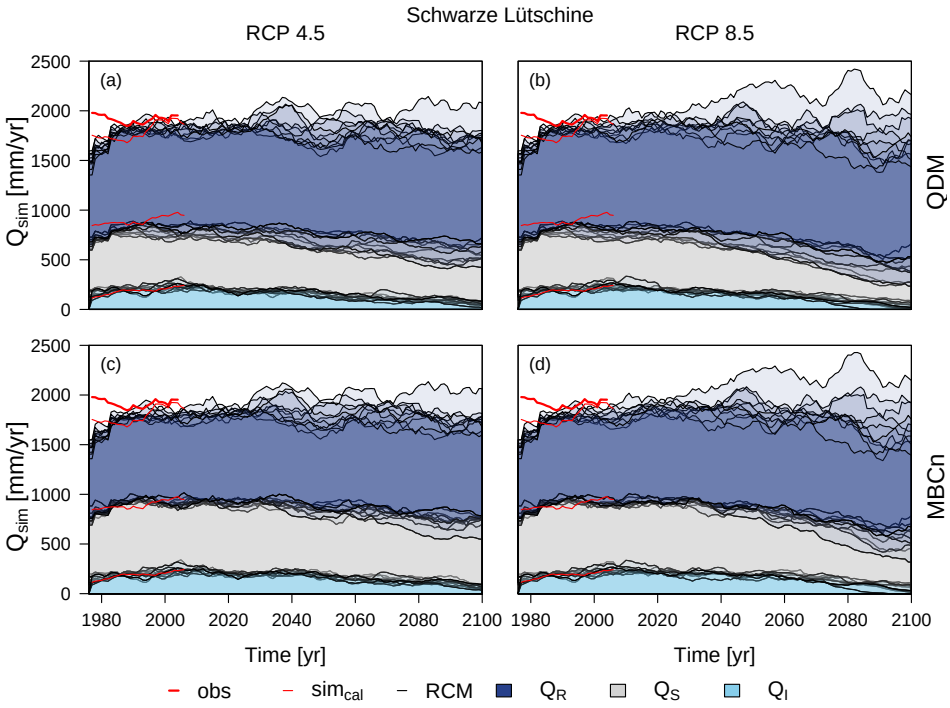

Figure A20: 11-year moving average of annual runoff sums (Schwarze Lütschine).

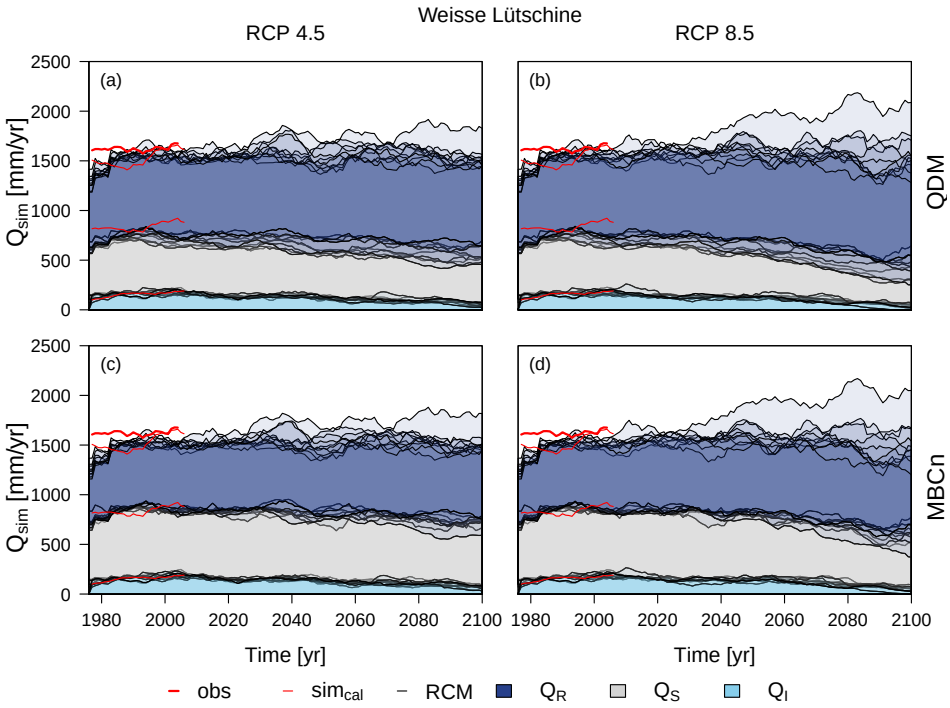

Figure A21: 11-year moving average of annual runoff sums (Weisse Lütschine).

C4 Runoff regimes

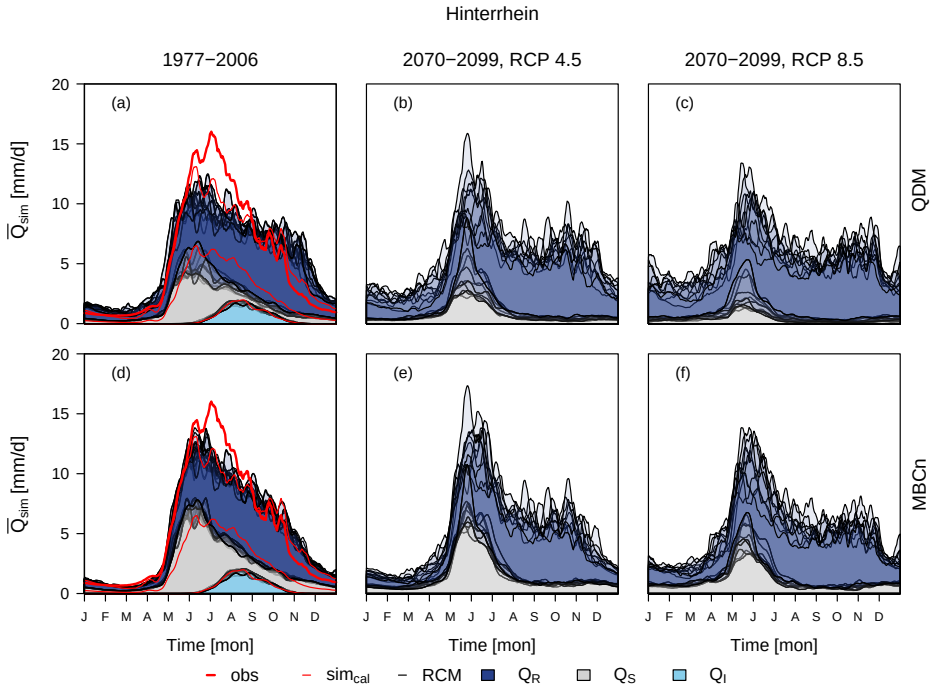

Figure A22: Runoff regimes using 11-day moving averages of daily runoff (Hinterrhein).

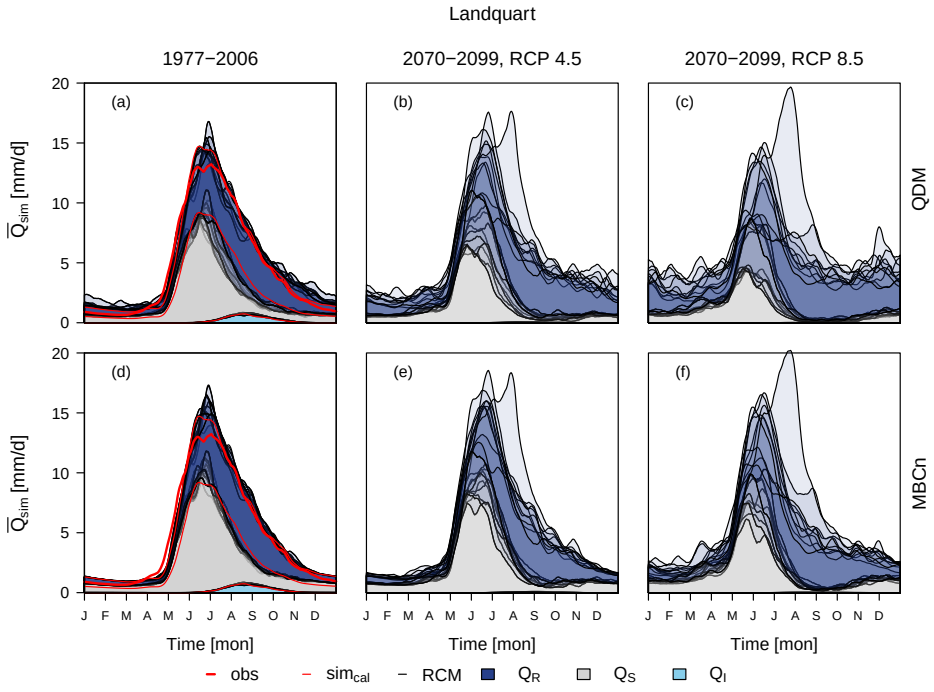

Figure A23: Runoff regimes using 11-day moving averages of daily runoff (Landquart).

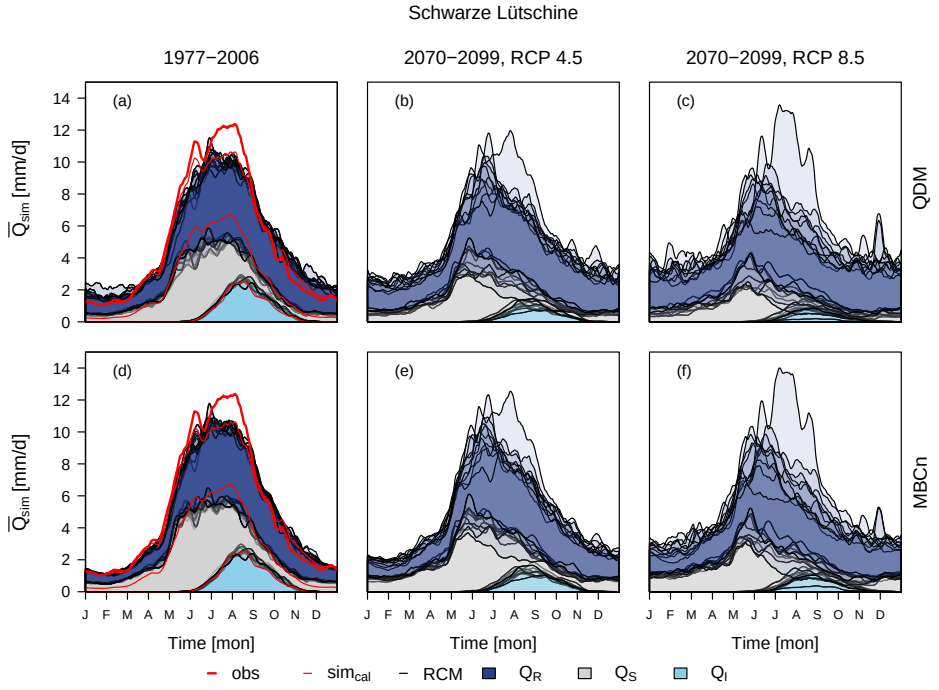

Figure A24: Runoff regimes using 11-day moving averages of daily runoff (Schwarze Lütschine).

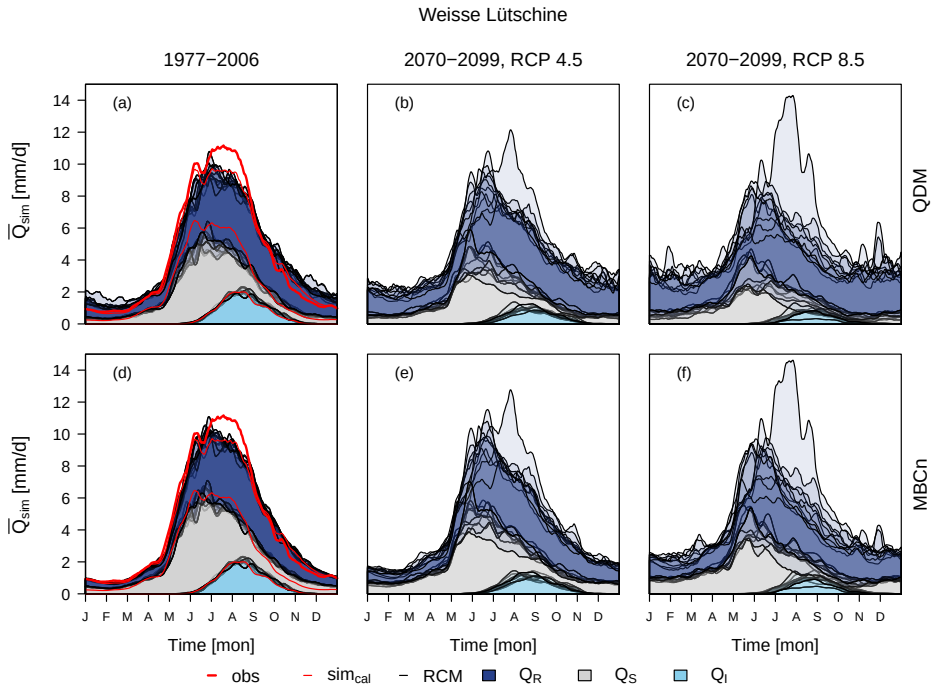

Figure A25: Runoff regimes using 11-day moving averages of daily runoff (Weisse Lütschine).

Ehrenwörtliche Erklärung

Ich erkläre, dass ich die Arbeit selbstständig angefertigt und nur die angegebenen Hilfsmittel benutzt habe. Alle Stellen, die dem Wortlaut oder dem Sinn nach anderen Werken, gegebenenfalls auch elektronischen Medien, entnommen sind, sind von mir durch Angabe der Quelle als Entlehnung kenntlich gemacht.

Freiburg, 29. September 2017

Judith Meyer